T.C.

ISTANBUL AYDIN UNIVERSITY

INSTITUTE OF GRADUATE STUDIES

INVESTIGATION OF DIFFERENT METHODS FOR LOAD SHARING AND POWER MANAGEMENT IN A HYBRID MICRO-GRID

M.Sc. THESIS

Hasibullah Shams

Department of Electrical & Electronic Engineering

Electrical and Electronics Engineering Program

April 2020

T.C.

ISTANBUL AYDIN UNIVERSITY

INSTITUTE OF GRADUATE STUDIES

INVESTIGATION OF DIFFERENT METHODS FOR LOAD SHARING AND POWER MANAGEMENT IN A HYBRID MICRO-GRID

M.Sc. THESIS

Hasibullah Shams

(Y.1613.300019)

Department of Electrical & Electronic Engineering

Electrical and Electronics Engineering Program

Advisor: Prof. Dr. Murtaza FARSADI

April 2020

DECLARATION

I hereby declare that all information in this thesis document has been obtained and presented in accordance with academic rules and ethical conduct. I also declare that, as required by these rules and conduct, I have fully cited and referenced all material and results, which are not original to this thesis.

Hasibullah Shams

Dedicated to My Lovely Father and Mother.

FOREWORD

In the name of Almighty ALLAH, the most merciful the most gracious, and may Allah's Peace and blessing be upon our Prophet MUHAMMAD P.B.A. Alhamdulillah after thanking to almighty Allah our creator, I would like to thank my Respectable Family specially My Father and Mother who raised me to become a good person, they always supported me and believed at me, Encouraged me and gave me the strength while I was totally lost. They were patient during my mistakes and my bad times. Today what I have accomplished is because of their effort. I hope I can make them proud and return even some of what they gave me during their Entire lives.

I would like to thank my thesis advisor Prof Dr. MURATZA FARSADİ for his guidance, support, and help during my work in the thesis. I thank him for everything I learned from him.

I thank all my teachers starting from my school time until today as they had great influence on me and made me love education and I hope I can become one day a good teacher as they were

April, 2020   **Hasibullah Shams**

(Electrical and Electronics Engineer)

TABLE OF CONTENT

ABBREVIATIONS

AC	**:**	Alternation Current
DC	**:**	Direct Current
DERS	**:**	Distributed Energy Resources
DG	**:**	Distributed Generation
EMS	**:**	Energy Management System
ESS	**:**	Energy Storage System
ESUs	**:**	Energy Storage Units
MG	**:**	Microgrid
MPPT	**:**	Maximum Power Point Tracking
MS	**:**	Microsystem
PCC	**:**	Point of Common Coupling
PID	**:**	Proportional Integral Derivative
PSF	**:**	Power Signal Feedback
PV	**:**	Photovoltaic Panels
PWM	**:**	Pulse Width Modulation
SC	**:**	Solar Cell
SOC	**:**	State of Charge
SOGI	**:**	Second Order Generalized Integrator
SPU	**:**	Single Phase Uni
THD	**:**	Total Harmonic Distortion
TPU	**:**	Three Phase Unit

LIST OF FIGURES

LIST OF TABLES

INVESTIGATION OF DIFFERENT METHODS FOR LOAD SHARING AND POWER MANAGEMENT IN A HYBRID MICRO-GRID

ABSTRACT

A grid consists of a set of distributed generation units, energy storage resources, communication links and local loads, and can operate in two modes connected to the grid and separate from the grid. Power management and load sharing between grid units in a separate mode can be in both centralized or decentralized. In a decentralized way, with decentralized method is preferable due to local measurements, and the lack of a fast communication link and reliability.

In this thesis, a micro grid consisting of distributed generation units of a solar type and a storage source of a kind of battery is considered that can be connected independently (by separate inverters) or in combination of PV / battery (by a common inverter) to the grid. The purpose of this thesis is to provide a power management method and a decentralized load distribution for offshore grids, consisting of a variety of independent solar panels, independent batteries, and solar / battery combinations. In the proposed method, the operation of each grid unit is divided into six states and, depending on the different conditions, each unit operates in one of these situations. The control of the solar cells, the battery and the inverter unit vary according to the performance status. In this method, only the local measurements of the conditions of change are examined. The automatic balancing of battery charge rates and the optimal use of solar array capacity to supply power and charge the batteries is one of the most important features of this method. This method is firstly investigated for a single-phase grid, and then generalized to a single-phase / three-phase mixed-grid grid in which single-phase units are connected to different phases of a three-phase grid. Power transmission from phase to another phase and supplying the charge or charge power of a phase from another fuzzy is a feature of this method in single-phase / three-phase combination mode.

Keywords: *Microgrid, decentralized power management, hybrid PV battery units, hybrid single/three-phase microgrid, PV power curtailment, SoC.*

HİBRİT MİKRO GRİDDE YÜK PAYLAŞIMI VE GÜÇ YÖNETİMİ İÇİN FARKLI YÖNTEMLERİN İNCELENMESİ

ÖZET

Şebeke, bir dizi dağıtılmış üretim ünitesi, enerji depolama kaynakları, iletişim bağlantıları ve yerel yüklerden oluşur ve şebekeye bağlı ve şebekeden ayrı olarak iki modda çalışabilir. Ayrı bir modda Mikro Şebeke üniteleri arasındaki güç yönetimi ve yük paylaşımı hem merkezi hem de merkezi olmayan olabilir. Merkezi olmayan bir şekilde, yerel ölçümler ve hızlı iletişim bağlantısının ve güvenilirliğinin olmaması nedeniyle merkezi olmayan yöntemle tercih edilir.

Bu tezde, Microgrid bir güneş türü ve (ayrı inverter) veya PV / batarya ile bir kombinasyon halinde, bağımsız bir şekilde bağlanabilir olduğu düşünülmektedir bataryanın bir türden bir saklama kaynağı dağıtılmış üretim birimlerinin oluşturduğu (ortak bir inverter tarafından). Bu tezin amacı, çeşitli bağımsız güneş üniteleri, bağımsız batarya ve güneş / batarya kombinasyonundan oluşan ağ mikro şebekeleri için yeni bir merkezi olmayan güç yönetimi ve dağıtım yöntemi sağlamaktır. Önerilen yöntemde, her bir şebeke ünitesinin çalışması altı duruma bölünür ve farklı koşullara bağlı olarak, her birim bu durumlardan birinde çalışır. Güneş pillerinin, akünün ve evirici ünitesinin kontrolü performans durumuna göre değişir. Bu yöntemde, değişiklik koşullarının sadece yerel ölçümleri incelenir. Pil şarj oranlarının otomatik olarak dengelenmesi ve pilleri beslemek ve şarj etmek için güneş enerjisi dizisi kapasitesinin optimum kullanımı bu yöntemin en önemli özelliklerinden biridir. Bu yöntem ilk olarak tek fazlı bir şebeke için araştırılır ve daha sonra tek fazlı ünitelerin üç fazlı bir şebekenin farklı fazlarına bağlandığı tek fazlı / üç fazlı karışık ızgaralı şebekeye genelleştirilir. Fazdan başka bir faza güç iletimi ve bir fazın başka bir bulanıktan şarj veya şarj gücü sağlanması, bu yöntemin tek fazlı / üç fazlı kombinasyon modunda bir özelliğidir.

Anahtar Kelimeler: *Mikro şebeke, merkezi olmayan güç yönetimi, hibrit PV pil üniteleri, hibrit tek / üç fazlı mikro şebeke, PV güç azaltımı, SoC*

1. INTRODUCTION

Due to the lack of fossil fuels and related environmental issues, the attractiveness of using renewable energy sources or renewable energies are increasing day by day. These sources are often exploited as distributed generations units. It is possible that distributed generation units operate in two ways both: connected to the grid and separated from the grid or islanded mode. In islanded mode; the distributed generating units have no connection to the main grid and feed local loads. In this case, using energy-saving sources such as batteries, the balance between production and energy consumption is established. In grid connected mode, the distributed generating units are connected to the main grid and the power is injected into the grid.[1]–[4]. According to current standards, the distribution network for the operation of the grid-connected distributed generation systems, in the event of disconnection of the main grid, the distribution sources must be separated from the grid within a maximum of 2 *seconds* [5]. This way, loads placed in the disconnected area of the grid, where there is also a scattered power supply, will remain powerless, and the scattered power source will not be powered until the main grid is reconnected. To use the capacity of distributed generation units at the time of disconnection of the main grid, the idea of using a micro-grid has been proposed. A micro grid consists of a set of distributed generation units, energy storage resources, communication links, and local loads. Distributed generating units are usually connected to the grid using an electronic power converter which provides much flexibility in controlling and managing the micro-grid. In a micro-grid, hardware and resource control systems are designed to be able to inject power in both connected and separate states [6]. Due to the micro-network (MG) capability of continuity of power supply when the main network is disconnected, the most important feature of the micro-network (MG)is its significant increase in reliability compared to conventional networks (Grids). As a result, the use of microgrids in power supply to critical and sensitive loads is increasing steadily, and as the world continues to develop into more energy

efficient storage systems and lower prices, the world's electricity distribution networks will move toward microcontrollers (Microgrids) . Distributed generators (DG) in terms of technology can be into three categories as Fossil fuels, Renewable energy and Energy storage devices. Gas turbines and microturbines use fossil fuel gas and can be used to generate electricity and heat at the same time. Renewable energies include Wind and Solar (photovoltaics), Geothermal and other types and their use is increasing day by day due to the lack of environmental pollution. Batteries, supercapacitors, and water storage dams are used as energy storage [7]. Among renewable energy sources, solar energy has received a great deal of attention due to the need for non-mobile mechanical installations, pollution free energy generation process and low maintenance cost [8]. The most important factor in preventing the spread of solar energy use is its high initial cost but given the day-to-day technology of solar cells and the reduced cost of manufacturing and increasing their efficiency, the introduction of new structures at lower cost and higher efficiency for solar converters. And with the significant increase in solar system reliability, solar energy is expected to make up a significant share of electricity generation [3]. According to the European Solar Associatio[1] [European Photovoltaic Industry Association(www.epia.org)] in the year 2015 the total installed solar capacity worldwide has exceeded 200 GW and solar power is capable of accounting for 15% of Europe's total electricity generation by 2030. Also, if only 0.7% of Europe's land is covered by solar cells, Europe's total electricity demand will be met. Due to the expansion of the use of small domestic solar units in the distribution network as well as the necessity of using batteries alongside them to prevent severe fluctuations due to the variability of solar power produced by future standards is not unthinkable soon to be able to utilize micro-grids for home solar panels. Therefore, the overall aim of this thesis is to present new control methods for solar-powered micro-grids.

1.1 Issues Raised In Solar Microgrids

There are various issues in PV solar micro-grids, each of which has been devoted to extensive research. Some of these issues exist in all micro-grid networks, whether solar or other sources, and some are solely for PV solar

micro-grids. These issues can also be addressed in two general categories at the whole micro-network level or at the level of each micro-grid unit.

1.2 Operation Method

Some Micro-grids are only used as islanded separately from the grid, while others are used in both connected and isolated states. When connected to the grid, the voltage and frequency at the point of common coupling (**PCC**) are imposed by the main grid and the micro-grid controller controls the active and reactive power exchanged with the main grid. In islanded mode, because the micro-grid has no connection to the main grid, the amplitude and voltage frequency of the micro-grid should be determined automatically by the distributed generation or energy storage sources within the micro-grid.

1.2.1 Maximum power point tracking (MPPT)

Since the energy of the PV cells varies in different conditions and depends on the environmental conditions and the amount of radiation, the maximum power point tracking (MPPT) methods must be used to extract the cells at any time as much as possible. There are many methods for tracking the maximum power point (MPPT) that use a particular solar cell's voltage-voltage curve [8]–[13]. The curve at different radiation levels for a particular solar panel is shown in Figure 1-1. In most of these methods, the maximum power point is detected by changing the solar cell voltage and observing the power changes.

The most important debate in the (MPPT) is tracking the maximum power point in partial shadow conditions. These conditions occur when part of the cells that are aligned or parallel to each other are in the shade, resulting in a P-V curve such as Figure 1-2 having more than one local maximum point. In this case, algorithms must be used to find the local maximum point with the maximum value (absolute maximum).
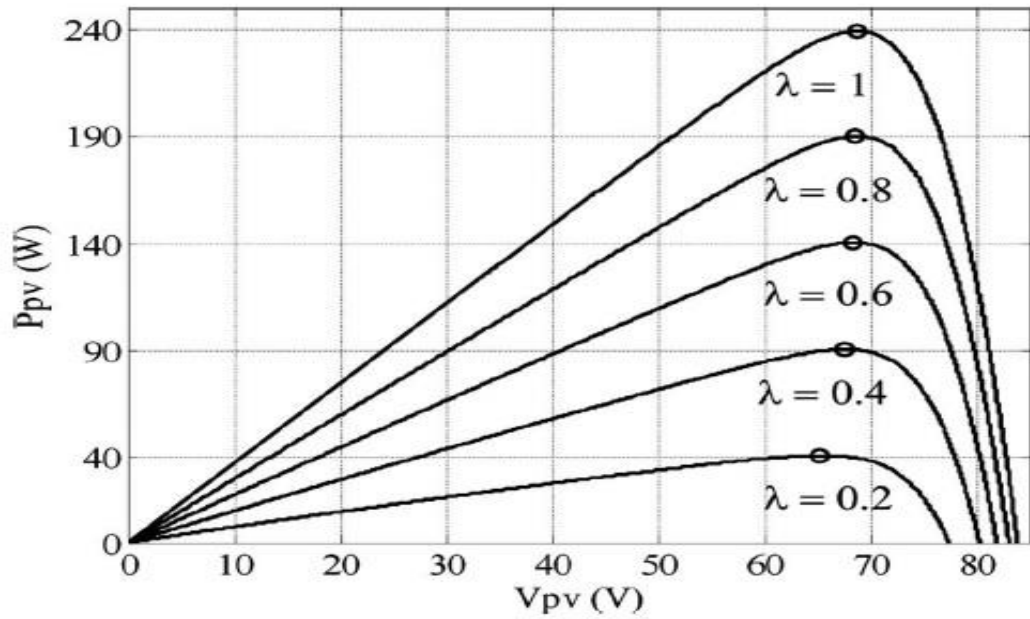
Figure 1.1: The **P-V** curve at different radiation levels for a solar cell.
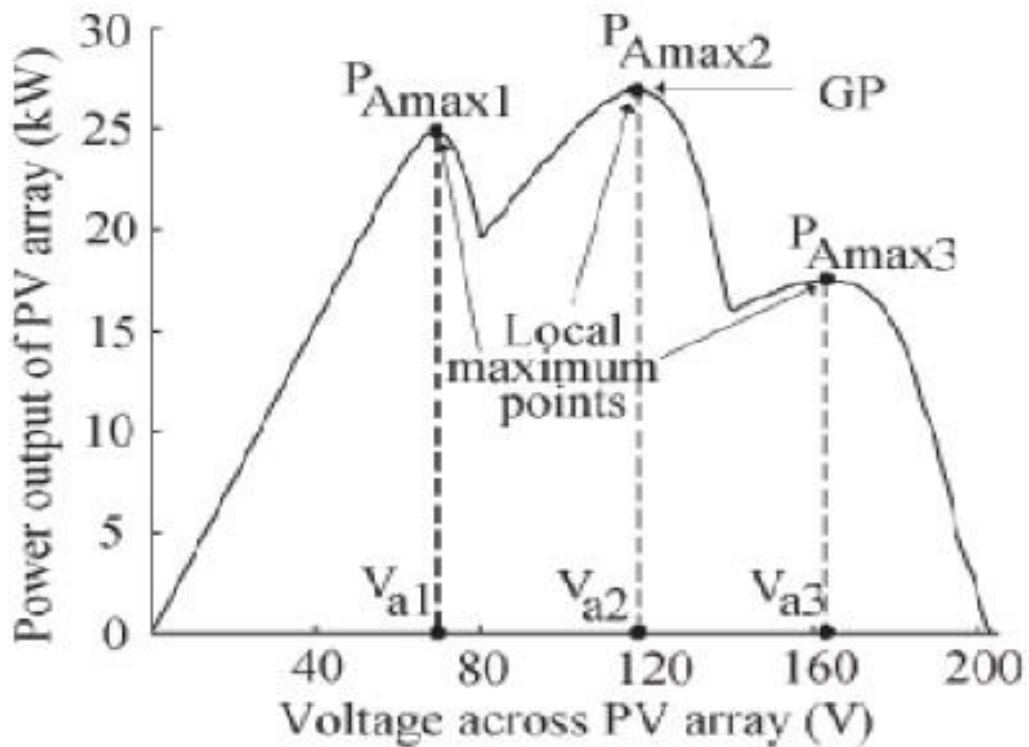
Figure 1.2: The **P-V** curve at partial shade conditions.

1.2.2 Energy storage

Due to the variability of the energy produced by a PV solar cell, in some applications, both the grid connected and separated (stand-alone) require an energy storage element such as a battery. The use of energy storage poses

challenges in how to manage power between the solar cell, energy storages and the consumer [14]–[19]. In off-grid applications, given that solar cell energy is zero during the night and highly variable during the day due to radiation conditions and environment temperature that is, the energy storage element such as the battery must be used to continuously supply the local load required. Under such circumstances, each time the solar energy exceeds the load, the surplus energy is stored in the battery, and each time the solar energy is lower than the required load, the rest is supplied from the battery. In some applications to increase system dynamics, in addition to the battery, the capacitor 1 is also used to respond to rapid power changes. In some applications connected to the grid, the storage element is used to prevent large variations injections to the grid. Due to the ever-expanding use of solar energy in the power system, large and rapid changes in grid energy may cause problems for the power system. You can use a power saver like a battery to solve these problems.

1.2.3 The structure of the solar converters

In a separate mode from the grid, since the battery is usually used, the structure must be used which has two input ports for connecting the solar cell and the battery. This can be achieved through a two-class structure including inverter and dc-dc converter with two input ports, or through newer structures that allow two or more inputs to be connected to a single-class structure. Two important classes of new structures, the cascade multilevel inverter (CHB)[1] (Cascade H-Bridge) [15], [20] and Z-Source Inverters [21], [22]. When connected to the grid, if the battery is used, the same issues are mentioned as in separate from of the grid. But the most important issue in this case is the issue of leakage current due to the scattering capacitance between the positive and negative terminals of the solar cell with the earth. If the transformer is used in the solar converter - whether the high frequency transformer in the DC-DC converter class or the low frequency transformer in the converter output - there will be no leakage current problem. But due to the bulk of the transformer, the higher cost and the relatively lower efficiency of the transformer structures, the market trend is towards using non-transformer structures. In this type of structure, specific structures should be used to prevent leakage current, or only certain specific

switching algorithms (such as bipolar switching in single-phase H-bridge converter) should be used [23]–[27]. The type of filter used in the converter is determined by application and can be of type L, LC, LCL or can be more complex structures like LLCL [28]–[30]. However, the LC filter is usually used in off-grid mode and the L or LCL filter in grid connected mode. Due to the better performance of the LCL filter in reducing the ripple switch current and its better dynamics, this type of filter is used more. But the most important problem LCL filter which is a tertiary filter, there is resonance. If this resonance is triggered by the frequency response of the LCL filter by a control loop or external perturbations such as network voltage perturbations, it may cause perturbations in the output current or even system instability. If this resonance is triggered by the frequency response of the LCL filter by a control loop or external disturbances such as grid voltage perturbations, it may cause disturbances in the output current or even system instability. Two main methods of passive damping and active damping are used to attenuate this resonance. In the passive damping method, a resistor with series capacitors is filtered. There are many ways to enable active attenuation, including multilevel control and active attenuation based on software filters [29], [31]–[35].

1.2.4 Connection of batteries and PV panels

Batteries and solar arrays can be connected to the micro-grid in two ways [18], [36].

1- Standalone: In this case, the batteries and solar arrays are connected to the micro-grid by two separate inverters.

2- Combined: In this case, the battery and the solar array have a common inverter, each connected to a common dc link by a dc-dc converter. The advantage of this structure is its lower cost and higher efficiency.

1.2.5 Control and power management of the micro-grid

In grid-connected mode, the usual way of controlling renewables like solar is to do so, as all sources generate maximum power and are injected into the main grid. But considering expanding the use of renewable resources, other functions such as reactive power control, energy management during hours of the day to

reduce the pressure on the main grid, and… are created for the micro-grid while its connected to the main grid. For example, during the daytime hours where consumption is low, generated energy by resources can be stored to the batteries and at the peak hours of consumption, by using the energy stored in the battery we can reduces the pressure on the main grid and reduces the maximum power to its medium power ratio. for this purpose, an overhead central controller or (Tertiary Controller) can be used to manage the actual and reactive power exchanged with the main grid. other functions, such as active filtering of nonlinear loads and power factor correction, can also be added to existing micro-grid. The most important challenge in the island state is how to allocate power between resources and their energy storage elements and their optimal management. Due to the absence of the main grid, the control of the amplitude and frequency of the voltage and the active and reactive power supply of the local loads is the responsibility of the micro-grid. In general, the power management method is divided into two categories:

1.2.5.1 Centralized and decentralized methods.

- Centralized Method: In this method, all information on energy sources, energy storage and loads in the grid is transmitted to a central controller via communication links and the central controller determines the amount of production or storage per unit. The most important problems with this method are:

- High cost and complexity due to the use of high bandwidth communication links.

- Low reliability due to dependency on proper communication links performance. In this case, if the communications links are broken, the power management will not work properly and may cause the entire network to fail.

- Adding or removing a unit in the grid requires changes to the central controller.

- Decentralized Method: In this method there is no central controller and all units (production, storage and controllable loads) are controlled independently by local measurements only, and no other unit information

7

is required. In this method the role of each of the distributed units is the same as the other units, and none of them have a more central role. It also provides greater reliability due to the lack of need for a central controller and communications links. It is worth to mention that in a decentralized method, a central controller with a low bandwidth link can be used to improve system performance, but unlike the centralized method, communication link failure does not cause system failure.

1.2.6 Grid structure

Depending on the needs of the micro-grid and types of loads available, the micro-grid structure can be in one of single-phase, three-phase, or a single-phase / three-phase combination. In the hybrid structure, single-phase loads and generating units are connected to different phases of a three-phase micro-grid.

1.2.6.1 Goals and approaches of the thesis

The purpose of this thesis is to present a new decentralized method of Active power management and load distribution in grids which are separate from the solar grid. Unlike previous research, the proposed method is not limited to micro-grids consisting solely of solar and battery independent units, but it is also applicable to micro-grids consisting of a variety of PV, independent batteries, and combined PV / battery units. This method maximizes solar power usage and the charge distribution between units is such that over time, the charge status of all the batteries in the micro-grid is balanced. The basis of the proposed method is a generalized Drupal method that changes its coefficients according to different performance states. Droop method is used to divide the reactive power.

1.2.6.2 Structure of the thesis

In the second chapter, the single-phase micro-grid is considered separately from the hybrid source network and details of the decentralized power management method are presented. This chapter describes the general modes of micro-grid operation, the different operating conditions of each micro-grid unit, how to control the batteries, PV solar and units per unit status of the inverters, the conditions for switching per unit and the startup algorithm for each unit are explained. Also effect of the impedance of the line connecting units on power

management is also investigated. At the end of the chapter, simulation and practical results are presented for a single-phase micro-grid consisting of three hybrid units. In Chapter three, the proposed method is extended to a single-phase / three-phase hybrid micro-grid. In this chapter, other conditions that do not exist in single-phase units are presented for the three-phase units and the transfer of automatic power from phase to phase is examined. At the end of the chapter, simulation and practical results are presented for a micro-grid consisting of a three-phase unit and two single-phase units connected to two phases of a three-phase unit. finally, in the fourth chapter, the results of the thesis are summarized and suggestions for further work are presented

2. DECENTRALIZED ACTIVE POWER MANAGEMENT IN SINGLE-PHASE HYBRID SINGLE-SOURCE MICROGRID

2.1 Introduction

The purpose of this chapter is to present an active power management and decentralized load distribution method for a single-phase micro-grid separate from the grid with different solar, battery and solar / battery units, such as shown in figure 2-1.
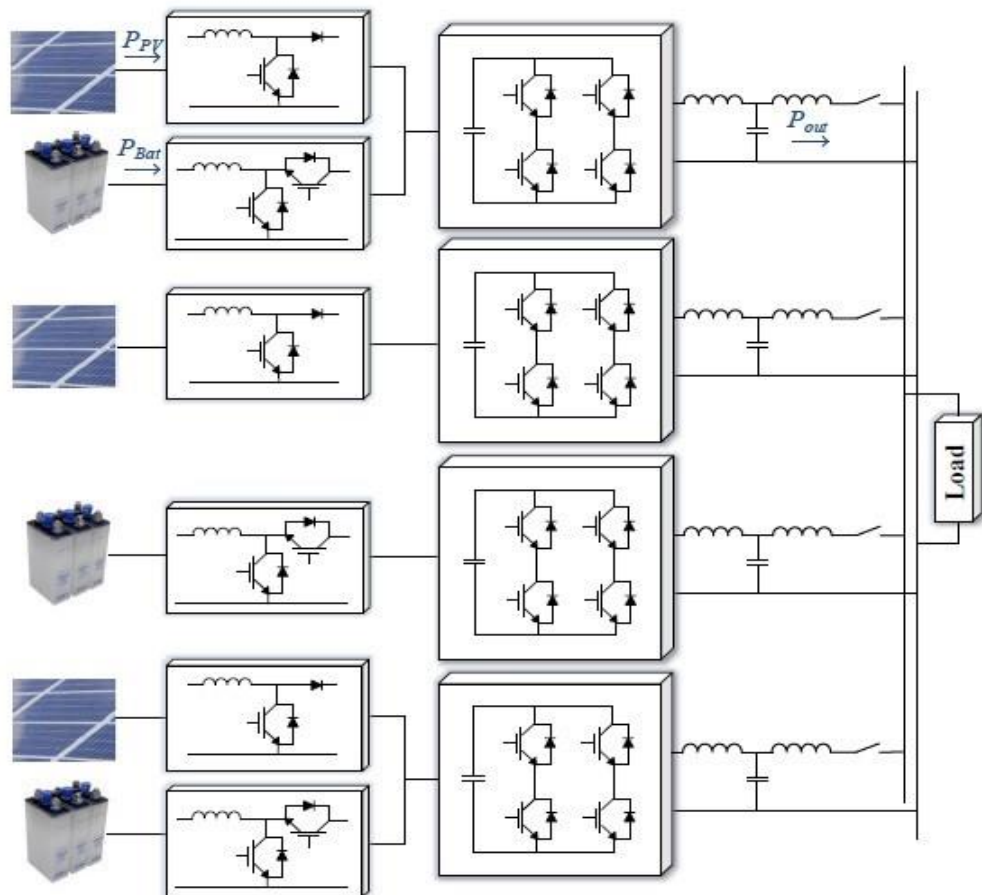
Figure 2.1: Typical single-phase MG structure.

This microgrid consists of three types of units:

1. Independent Solar (PV) Unit: In this type of unit, a set of solar cells are connected to a dc inverter link by a one-way incremental converter.

2. Stand-alone Battery Unit: In this type of unit, a set of batteries are connected to the inverter dc link by a two-way adapter converter.

3. Solar / Battery Combined Unit: In this type of unit, the solar cells are connected to a common dc link by a one-way adapter and the battery by a two-way adapter. The advantage of this structure is the use of two separate inverters to connect solar cells and batteries, reducing the cost of components and increasing efficiency due to the possibility of direct battery charging by the solar cell [18], [36], [37].

In a separate mode from the grid, the purpose of power management is to divide the load power between the various units, considering the amount of solar power generation and state of charge of the (SOC) battery units [38], [39].a Centralized power management [40]–[45] or Decentralized power management techniques can be used for this purpose [36], [46]– [51]. Because of the dependence of the telecommunications link between the units, the reliability of the centralized methods is less, and their complexity is higher [49], [52]. In this section, only decentralized active power management techniques are presented for separate micro-networks and finally a new approach is presented. Given that the focus of this thesis is on active power management, the common method presented in the papers has been used to divide reactive power.

2.2 An Approach Of Decentralized Active Power Management Method

The hybrid source systems provided in the article [46], [53]–[57] are only for grid-connected applications. Also, the hybrid source systems presented in the single unit [54], [55], and power management within a single unit that feeds its local load are investigated. İn [47] a micro-grid consisting of one battery unit and several solar units is provided. In the proposed method as a Master/Slave, the battery unit plays a major role and communicates with the PV units and controllable loads by controlling the network frequency according to its **SoC**. The method of this relation is illustrated in Figure 2-2. In this method, when the battery SoC is allowed in the range, the frequency is controlled at the rated

11

frequency. In more **SoC**s, indicating that the battery has less capacity to absorb excess PV power, the frequency is linearly increased to reduce the low power PV units produced. When the SoC reaches its maximum, the frequency reaches its maximum frequency and the PV units are completely cut off. The same method is used to phase out controlled loads when the SoC of the battery is reduced outside the permitted range.
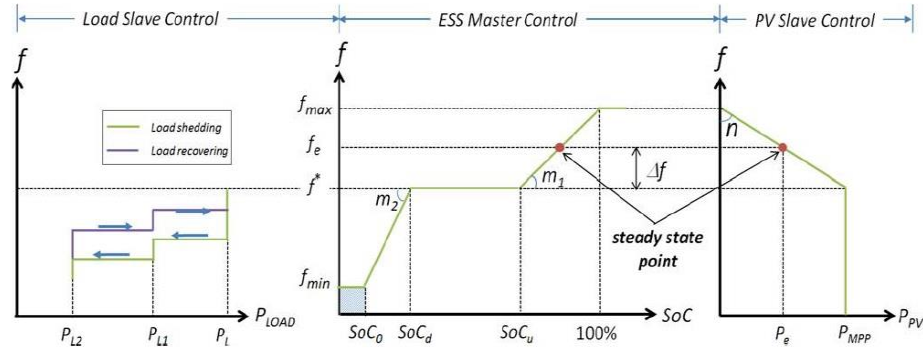
Figure 2.2: Frequency control method in [48].

One of the biggest disadvantages of this method used in SMA inverters is the possibility to use only one battery unit and this method cannot be used if there are more battery units in the micro-grid. Similarly, the method presented in [46], only applies to one battery unit. In [48], a micro-grid consisting of a single wind turbine unit and a single battery unit is shown in Fig. 2-3, which are spaced apart from each other.
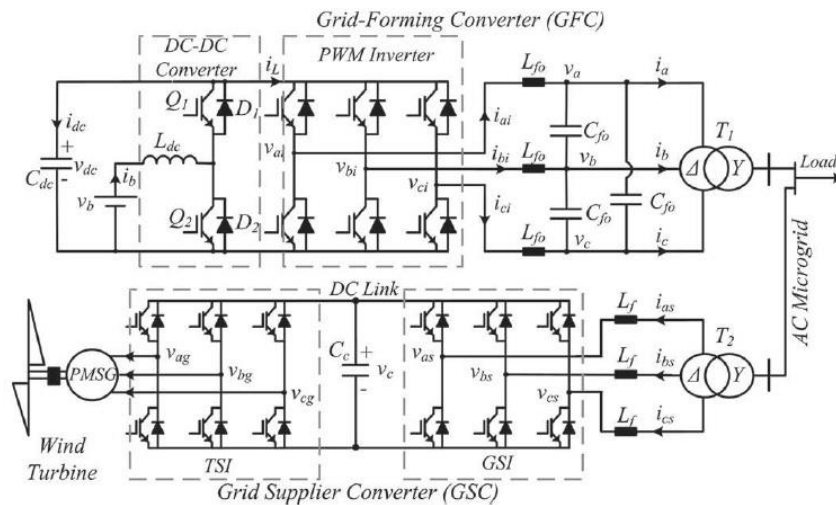
Figure 2.3: Micro-grid studied in [48]**.**

12

In [49], microbeads consisting of several standalone solar units and several standalone battery units are considered in figure 2-4 and a method for power management is presented.
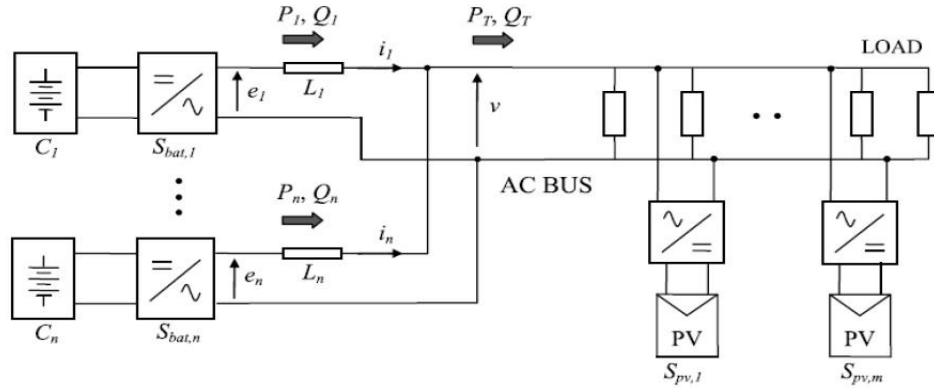
Figure 2.4: The micro-grid studied in [49].
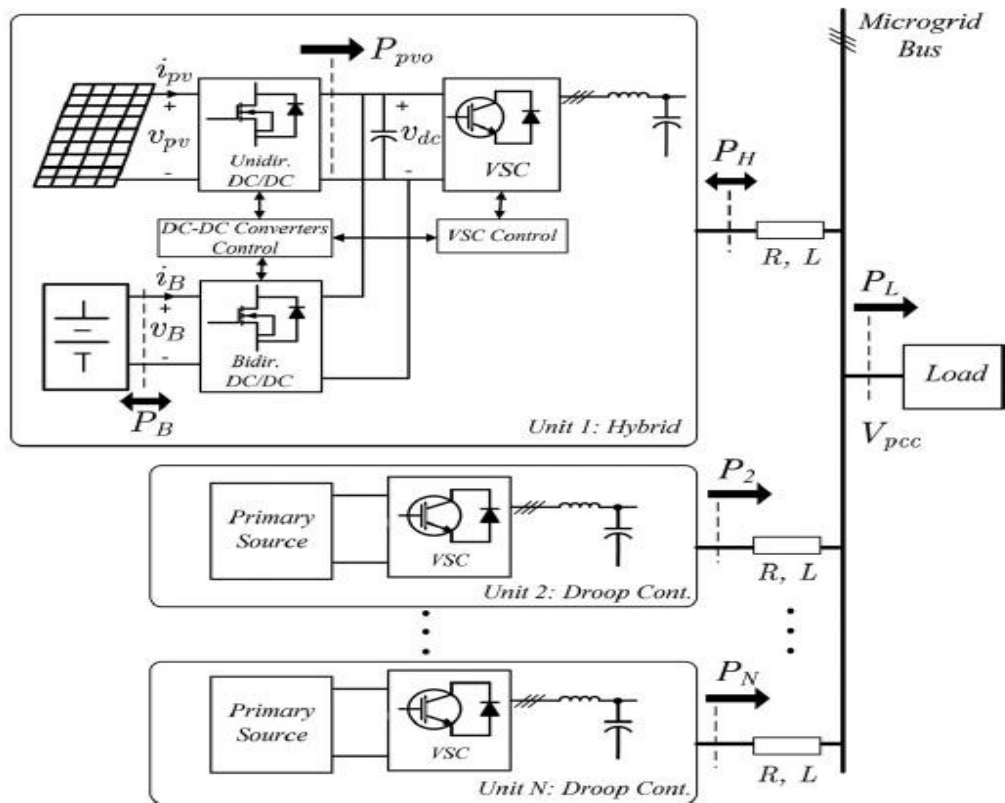
Figure 2.5: The microchannel studied in [36].

In this way, when a battery unit reaches its minimum SoC, that unit reduces its frequency by transferring more power from the batteries with a higher SoC.

Conversely, when a battery unit reaches its maximum SoC, that unit transmits power to batteries with less SoC by slightly increasing its frequency. Whenever all the batteries reach the maximum SoC, the frequency increases to the maximum frequency. In this case, the power of solar units should be reduced. The disadvantages of this method are the transfer of energy from one battery to another which reduces the overall efficiency of the system due to battery charge losses. Similarly, the methods proposed in [50] and [51] apply only to microgrids consisting of standalone battery units and PV.

In [36] a method for controlling a solar / battery unit connected to a microcontroller controlled by the Drop method is presented. This method assumes that a hybrid unit is connected to the microchannels controlled by a simple drop method and their source is unknown. The battery in the hybrid unit is responsible for supplying the load when other units in the micro-grid reach their maximum power. The application of this method is solely for the micro-grid consisting of only one hybrid unit. As seen in the literature review, the methods presented so far for managing microgrid power are applicable only to microgrids having one of the following modes:

1. - Only consist of one standalone battery unit and several standalone solar units.

2. Consist of several independent battery units and several independent solar units.

3. Only have one combination of solar / battery unit.

Until now, there is no decentralized way to manage load distribution in micro-networks containing multiple hybrid units. The main challenge in this type of micro-grid is that the PVs operate as far as possible at the maximum power point, the charge and discharge of the batteries are properly managed, the battery can be recharged from the PV of other units, reducing the PV power if needed Units should be balanced, and all these issues should be decentralized and purely local measurement. In this thesis, an active power management and charge sharing method for separate micro-networks is presented which, unlike the methods presented in previous research, is not limited to micro-networks consisting of independent battery units and PVs and can be implemented in

micro-networks of different types. It has PV units, batteries and one or more combination units.

The method presented in this thesis addresses all the above challenges without the need for a link between units and without knowing the amount of load, and has the following characteristics:

- Power management is possible in all micro-grids consisting of PV, battery and hybrid units.

- When the total charge of the micro-grid exceeds the maximum power of the PV unit, all PV sources in the micro-grid (standalone or hybrid) produce MPP (maximum power point) and all the batteries in the micro-grid (standalone or hybrid) generate overload. Also, the overload split between batteries is such that the battery with more SoC has more discharge power so that the batteries will eventually be balanced with SoC.

- When the maximum PV power of the units exceeds the total charge of the micro-grid but the batteries in the micro-grid have the capacity to absorb excess PV power, the batteries are charged by the PV excess power. Charging power between batteries is such that, with as little battery power as possible, it has a higher charge power so that the batteries will eventually balance the SoC.

- When the total maximum power of the PV units exceeds the total charge of the micro-grid and the batteries in the micro-grid are fully charged or have reached their maximum charge, the power output of some PV units is lower than the MPP point to balance production and consumption.

- In all cases, the limitations of the SoC and the maximum battery charge as well as the capacity of the inverters are considered.

This thesis assumes that all units and loads are owned by the unit and the goal is to optimize the overall performance of the micro-network. In this case, for example, if the PV power in a unit exceeds the local load capacity of the unit but the sum of the micro-grid PV power is less than the total micro-grid load power, the unit battery cannot be charged with a surplus PV power, but to

provide total power. The charge is charged. Also, if the total charge is less than the sum of the micro-grid PV power, the amount of battery charge per unit is not related to the PV value of that unit, but the total micro-grid power of the micro-grid is distributed between them in terms of capacity and SoC of the batteries and if in PV power units. Too little, the unit from the microgrid absorbs power and the unit's battery is charged proportionally to the other units. However, it is possible to modify the approach so that if the units are owned by different individuals, it can respond to new needs arising from ownership differences and even incorporate economic issues that are beyond the scope of this thesis.

Although all the analysis and results presented in this chapter are related to single phase micro-grids, the method can also be implemented for three-phase micro-networks without any restrictions. Chapter 3 presents the necessary changes to implement this approach in both single-phase / three-phase hybrid micro-grids.

2.3 Decentralized Active Power Management In Microgrid

In the proposed method, to manage the decentralized active power of microgrid, the total performance of the microgrid is divided into three general states. Also, according to the battery conditions, PV power and other conditions, the performance of each unit in the microgrid is divided into six states, each of which corresponds to one of the general modes of microgrid operation and has its own control conditions. What is important in controlling the units is the status of the unit and the state of the micro-grid resulting from the status of the units. In each situation, the type of control for each of the battery, PV and inverter components is different, for example in situation 1, the PV converter is controlled at the maximum power point and the battery converter controls the dc link voltage but in situation 3, the battery converter charges the battery. Limits the dc link voltage of the PV converter. It is important to emphasize that each unit at the start-up, only by local measurements (microwave voltage amplitude and frequency measurement), detects the overall state of the microcontroller's operation and adjusts its initial state accordingly and proceeds accordingly. Depending on the local conditions of the battery, PV, frequency, etc. will

change its status. For simplicity of presentation and overall results of the analysis, a microgrid composed of three units is considered. With the brief modifications to the control method described below, the proposed method can be extended to standalone battery and PV units. Complete block diagram of control of each microgrid unit to implement decentralized power management in Figure 2-6 is shown. As can be seen in the figure, only local measurements are used to control each unit in the microgrid. Each unit control consists of five main parts:

1. Controller of incremental PV converter

2. Battery boost converter control

3. Inverter control

4. Determining the initial state and setting up the unit

5. Study of the changing condition

Before describing the power management method, it is necessary to describe the details of the control of the PV adapter, battery adapter and inverter. Also, given that the basis of the proposed method is the Droop method, a brief explanation is given.
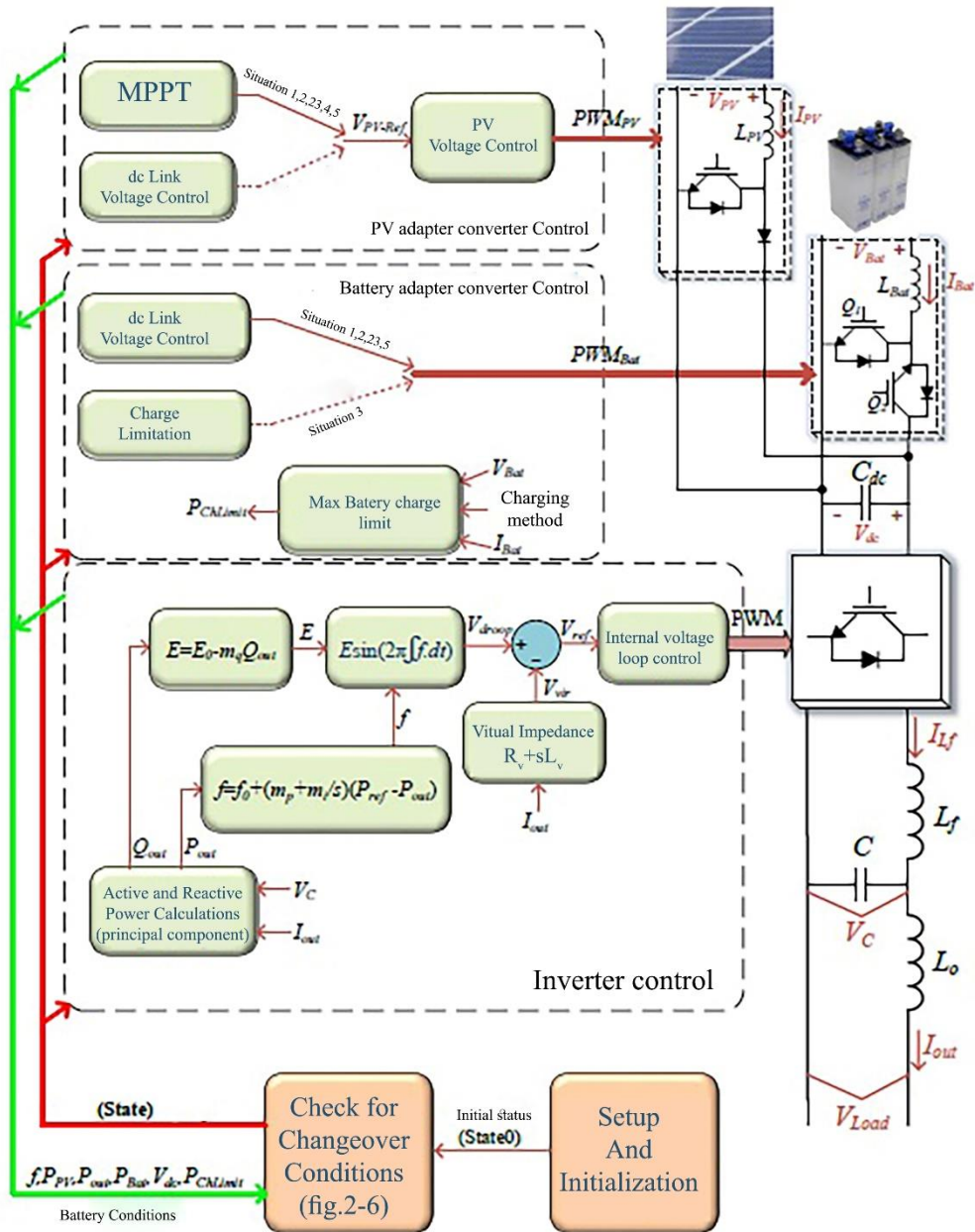
Figure 2.6: Block diagram of decentralized control of each microgrid unit

Table 2.1: Summary of the different status of a micro-grid unit

Status	1	2	2 & 3	3	4	5
Description	Maximum PV power and battery discharge	Maximum PV power and battery charge	Maximum PV power and battery charge limit	Reduced PV power and limited battery charge	Maximum PV power and disconnected battery	Maximum PV power and output power limit
Inverter control type	Voltage control (2-19)	Voltage control (2-25)	Power control (2-26)	Voltage control (2-29)	Power control (2-24)	Power control (2-23)
Battery control type	V_{dc} Control	V_{dc} Control	V_{dc} Control	Charging limit	Disconnected	V_{dc} Control
PV control type	Maximum power	Maximum power	Maximum power	V_{dc} Control	Maximum power	Maximum power
Corresponding Microgrid Mode	First	Second	second/third	Third	First	First
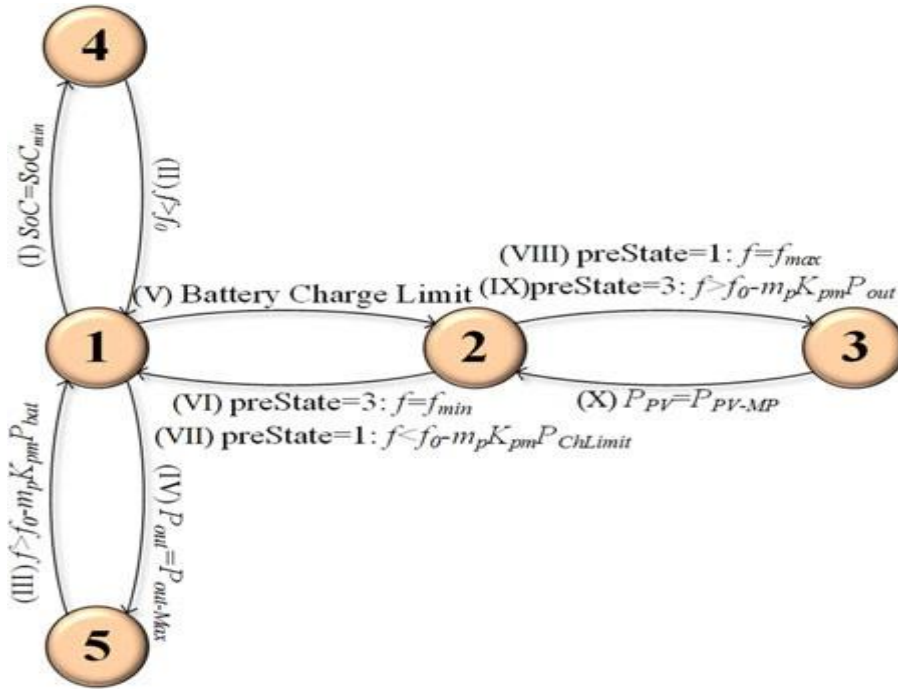
Figure 2.7: Conditions of Changing the Status of Each MG

2.3.1 Incremental PV converter control

Depending on the performance status of the unit as described below, the PV converter has two different roles:

In situations where PV must operate at the maximum power point, the task of the maximum power point tracking converter (MPPT) is a PV converter. as explained in the introduction to the dissertation, in most methods (MPPT), the maximum power point is detected by changing the voltage of the solar array and examining its output power changes. Therefore, in MPPT mode, the PV converter must follow the PV voltage reference set by the algorithm (MPPT). In these situations, the dc link voltage is controlled by the battery converter in the same amount.

In the situation 3, the task of the PV converter is to control the dc link voltage. In this situation, the solar array is operating at a power below the maximum power point. In this case, the output of the dc link voltage controller is the PV reference voltage. Given the P-V curve of a solar array in $Fig. 1-1$, the lower the voltage at which the maximum power ($V_{PV\text{-}MP}$) moves to the right, the lower the solar power. Therefore, the logic for controlling the dc link voltage is that if the V_{dc} was larger than the reference voltage, it would be necessary to reduce the injection power to the dc link by the PV, necessitating an increase in the V_{PV}

voltage relative to the voltage V_{PV-MP}. Of course, curves with multiple points do not always have these conditions. In this case, more complex controllers are needed to control (V_{dc}). Of course, if simple control is also used in these situations, there is no problem because if the controller fails to control (V_{dc}), the state changes to state 2,3 and at that point the original maximum power is detected and If the changeover condition is described below, the unit returns to status 3 again. The method of controlling the PV converter in both cases is shown in Fig 9-2. After the PV (V_{PV-ref}) reference voltage is determined by external MPPT loops or dc link voltage control, this reference voltage is followed by a dual-loop controller including external PV voltage control loop and internal PV current control loop. The method of determining the coefficients of the controllers is described in [36]. Since in all cases, an external loop specifies the PV voltage reference, there is no need to follow this reference precisely, so in this treatise after **V_{pv-ref}** is determined, the   Duty Cycle or (workload)of incremental converter is given by the following relation based on the output voltage ratio -The converter input is incremental, specified:

$$D_{PV} = \left(V_{dc} - V_{PV-ref}\right)\Big/V_{dc} \tag{2-1}$$
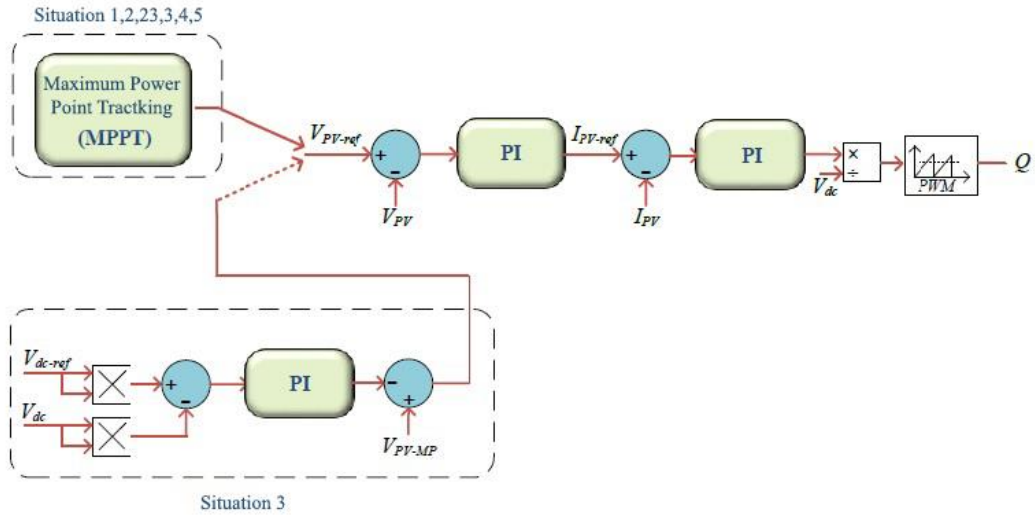
Figure 2.8: Control method of PV incremental converter in different situations

In this figure, V_{PV-MP} is the last peak voltage applied by the MPPT. Although this voltage varies depending on the environmental conditions and the radiation, the changes in the proposed power management method do not have a

significant impact. The reasons for not affecting $V_{PV\text{-}MP}$ changes will be described in the situation 3.

2.3.2 Battery boost converter control

Depending on the operating status of the unit, the battery adapter is controlled in two different modes:

In situations where PV works at maximum power point, the task of the battery converter is to control the dc link voltage at its reference value. In fact, in these situations, the battery maintains the power balance at the dc link and keeps the V_{dc} constant by supplying or absorbing the difference in PV power and unit output power. In situation 3, which controls the PV voltage of the dc link, the task of the battery converter is to control the battery charge in the charge limitation state. In this case the battery should be charged at the maximum possible power. There are several ways to optimally charge batteries, the most common being two-stage charging with constant current and constant voltage **(webpage)**. In this way, the battery is first charged by a constant current (I_{charge}) depending on the capacity and characteristics of the battery. Charging the battery increases its voltage continuously until the voltage reaches the maximum value specified by the manufacturer (V_{boost}). At this time, the battery voltage reference is kept constant and as a result the battery charge current decreases gradually. When the battery is fully charged, the charging current drops to zero, and the battery voltage reference is reduced to the nominal value of the battery voltage (V_{float}) which is specified by the manufacturer and it less than (V_{boost}) is specified. However, at the first charge of some types of battery, the voltage applied to the battery is more than the (V_{boost}) which is called ($V_{equalize}$).

The method of controlling the battery adapter converter in different situations is shown in Fig. (2-10) the method of determining the coefficients of the controllers is described in [48].
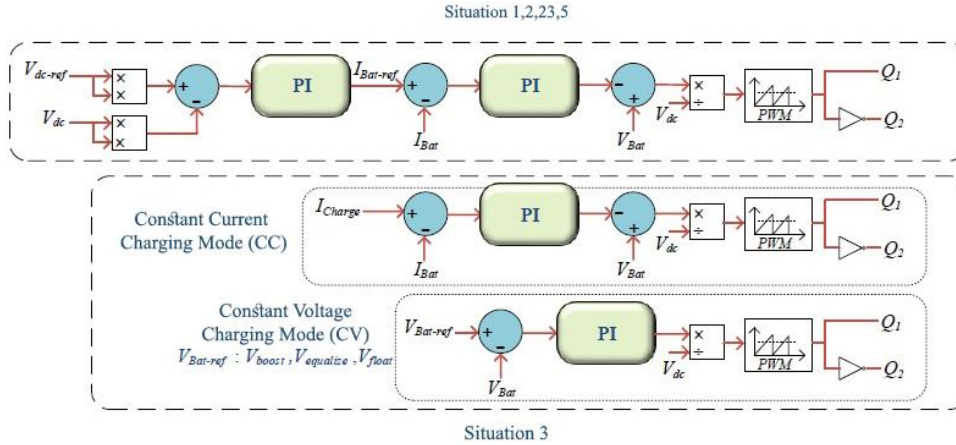
Figure 2.9: Battery boost converter control methods in different situations

As will be explained in the 2,3-mode description, the battery is also in the charge limit, but its charge is indirectly applied by adjusting the unit's output power.

In this case, the battery controls the voltage of the dc Link voltage, and for the battery to be charged at constant voltage or constant current, it is necessary to allow the battery charge to be set and the reference value of the output power equal to the PV power difference and the battery charge. The method for determining the battery charge power in each of the constant current and constant voltage modes is shown in Fig. (2-11). In this figure, $P_{chLimit} < 0$ is the battery power allowed.
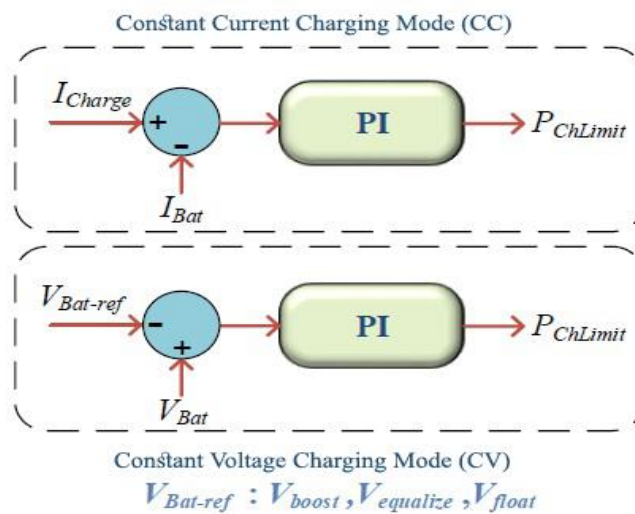
Figure 2.10: Method for determining the Battery Authorized Charging Power in situation 2,3.

2.3.3 Inverter control

As shown in the block diagram block (2-6), the inverter control of each unit consists of the following sections:

2.3.3.1 Active and reactive power output calculation

One of the methods of calculating the actual and reactive power in a single-phase system is to calculate the power by the following equations using the perpendicular voltage and current components.

$$P_{out-t} = \frac{1}{2}\left(V_\alpha I_\alpha + V_\beta I_\beta\right)$$ (2-2)

$$Q_{out-t} = \frac{1}{2}\left(V_\beta I_\alpha - V_\alpha I_\beta\right)$$

In these equations, V_α and I_α are Simultaneous phase values with output voltage and current, and V_β and I_β are instantaneous values that are 90 degrees with phase voltage and output difference. V_{out-t} and Q_{out-t} are the Instantaneous values of active and reactive power. Given a sinusoidal component with twice the original frequency at the instantaneous power calculated by (2-3), a low pass filter is used as below to calculate the average power.

$$P_{out} = \frac{\omega_f}{s + \omega_f} P_{out-t}$$ **(2-3)**

$$Q_{out} = \frac{\omega_f}{s + \omega_f} Q_{out-t}$$

There are various methods for generating a 90-degree phase difference signal compared to the original signal, which uses the **SOGI** (second order generalized integrator) method in this thesis. The block diagram of this method is shown in (2-12).
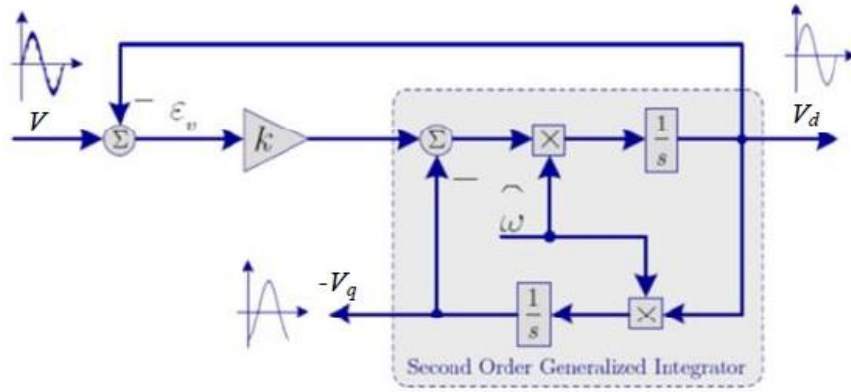
Figure 2.11: OSG perpendicular signal generation by **SOGI-OSG** method

The most important feature of this method is that by adjusting its coefficients, the main harmonics and the signal perpendicular to the main harmonics can be extracted, therefore, even for nonlinear loads and high-disturbance loads, one can only calculate the actual and reactive power of the main component of voltage and current.

2.3.3.2 Active and reactive power control

In order to determine the frequency and amplitude of the inverter output voltage, a method based on the Droop method is used. In this method, the output voltage reference range is determined based on the Q-E common drop relation, but the output voltage reference frequency is determined by a new method based on the modified P-f droop relation, which will be described in detail below.

2.3.3.3 Virtual impedance

This section can add a self-resisting virtual impedance to the inverter output. The virtual impedance resistor is used to increase the stability of the droop method and its inductor to increase the X/R ratio of the inverter output [58]. In Section 2-3-9, the effect of the inverter output impedance and impedance on the droop method is investigated.

To implement the virtual impedance, the corresponding voltage droop can be subtracted from the reference voltage value.

$$V_{vir} = R_v I_{out} + L_v \frac{dI_{out}}{dt} \tag{2-4}$$

Assuming the output current is sinusoidal, its derivative has a 90-degree difference from its original value, so the I_β value can be used to prevent the implementation of the virtual inductor to prevent the derivative from being implemented.

$$V_{vir} = R_v I_{out} - L_v \omega I_\beta \qquad (2\text{-}5)$$

It should be noted that in this respect, the virtual predecessor exists only at the original frequency. To implement the virtual inductor in other harmonics, the perpendicular component of the current in the desired harmonics can be used, which can be easily extracted by **SOGI** method.

2.3.3.4 Voltage control

By this section, it follows the output voltage reference voltage determined by the active and reactive power control section from which the virtual impedance voltage is lowered. To increase speed and improve control loop stability, the double-loop control voltage is used as an (2-13) shape.
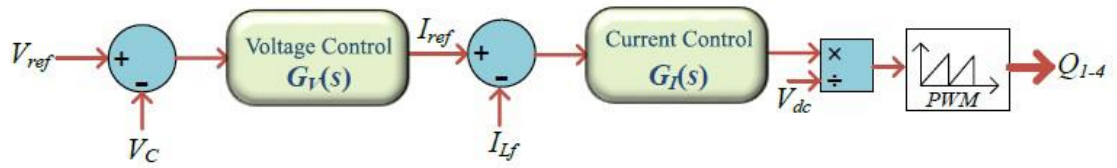
Figure 2.12: Inverter output voltage control loop

This control system consists of an external voltage control loop, Gv(s), and an internal current control loop, GI(s). For voltage and current control loops, linear controllers such as proportional-integral (PI) and proportional-resonant (PR) controllers are widely used because of their simple design and implementation. Due to the inability of the controller (PI) to follow the sinusoidal reference and the steady state error in amplitude and phase, most of the (PR) controllers are used.

The general structure of a (PR) controller is as follows:

$$G_c(s) = K_p + K_i \frac{\omega_c s}{s^2 + 2\omega_c + \omega^2} \qquad (2\text{-}6)$$

Where K_p, K_i and ω are proportional gain, integral gain, and controller resonance frequency, and ω_c is the frequency of the controller cutoff, which

reduces the sensitivity of the controller gain to the voltage reference frequency change. Compensation of different harmonics is possible through the combination of multiple proportional-resonance controllers. For this purpose, the compensator conversion function is considered as follows (PR+H):

$$G_c(s) = K_p + K_i \frac{\omega_c s}{s^2 + 2\omega_c s + \omega^2} + \sum_{h-3,5,7...} K_{ih} \frac{\omega_{ch} s}{s^2 + 2\omega_{ch} s + (h\omega)^2} \tag{2-7}$$

The conversion of this function as a chart is shown in Figure (2-14).
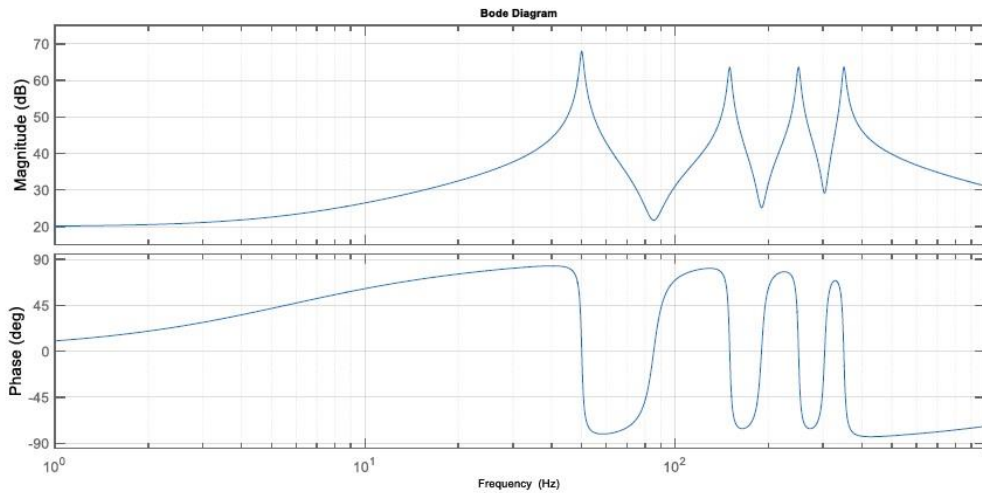
Figure 2.13: The graph chart of $G_c(s)$ with harmonic offsets of 3,5 and 7.

In the figure (2-14) a compensator (PR+H) is used for both voltage and current control loops. To determine the coefficients of the drives, the closed loop control diagram of the system is considered as (2-15), [59]. Since in closed-loop control, the capacitor voltage and the current of the inverter side of the inverter are controlled, the output filter type can be considered a filter (LC) with an output inductor of (L0).
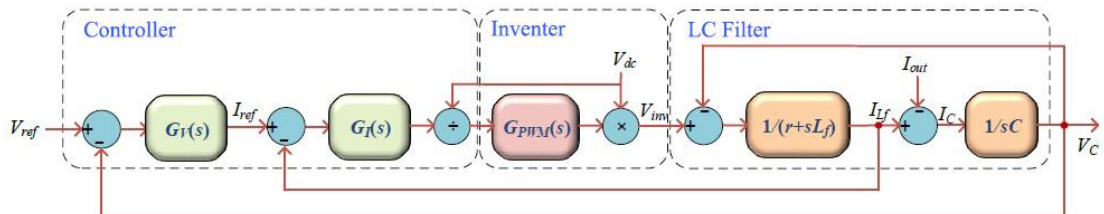
Figure 2.14: Inverter closed-loop control diagram

Using Mason's theory, the closed-loop voltage control function of the capacitor is written as follows:

$$V_c(s) = GV_{ref}.V_{ref} - Z_{out}I_{out}$$

$$= \frac{G_V(s)G_I(s)G_{PWM}(s)}{LCs^2 + rCs + (Cs + G_V(s))G_I(s)G_{PWM}(s) + 1}V_{ref}(s) -$$

$$\frac{r + Ls + G_I(s)G_{PWM}(s)}{LCs^2 + rCs + (Cs + G_v(s))G_I(s)G_{PWM}(s) + 1}I_{out}(s) \quad (2\text{-}8)$$

Which

$$G_{PWM}(s) = \frac{1}{1 + 1.5T_s.s} \qquad\qquad (2\text{-}9)$$

Is the Inverter conversion function, T_s is the Inverter sampling frequency and r is the resistive inductor of (Lf) filter The method of adjusting the coefficients of voltage and current compensators is fully described in [60]. Assuming the specification of table (2-4) and the compensation coefficients $K_{PI} = 5.6, K_{iI} = 300, K_{i3,5,7,9I} = 30, K_{pV} = 0.05, K_{iV} = 100, K_{i3,5,7,9v} = 50$ of the diagram were the conversion function $GV_{ref} = {V_c(s)}/{V_{ref}(s)}$ shown in Figure (2-16). As can be seen, the gain is the closed-loop conversion function of the desired frequencies 1 and its phase 0 indicating that the controller can follow the voltage reference exactly.
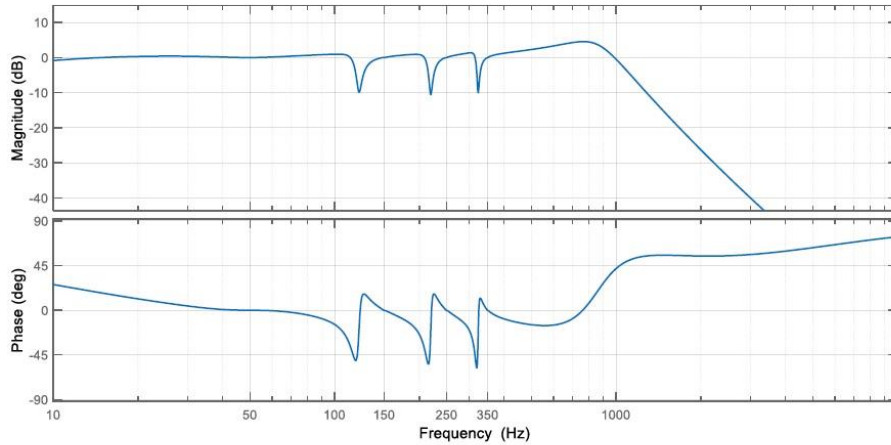
Figure 2.15: table chart of the closed loop conversion function of $GV_{ref} = {V_c(s)}/{V_{ref}(s)}$

The output impedance of the system, which is the output voltage for the perturbation current, is also shown in Fig 2-17. The small impedance at the desired frequency affects the effect of the output current reduces voltage control.
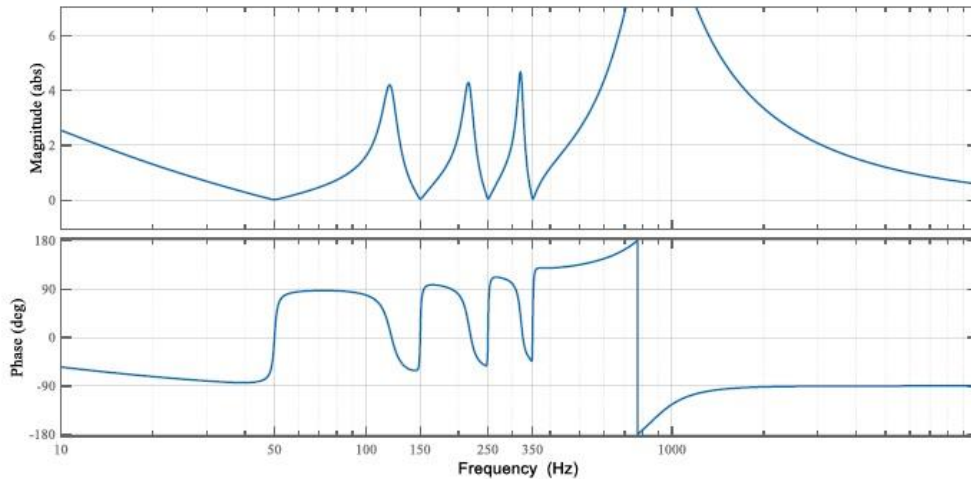
Figure 2.16: System output impedance in the frequency domain

2.3.3.5 An overview of droop method

The Droop method is one of the most common methods for dividing the active and reactive power between distributed generation units by decentralized method. To illustrate the Droop method, consider a few scattered inverter generating units connected to a common bus. Each unit can be modeled as an ideal series impedance voltage source as shown below.
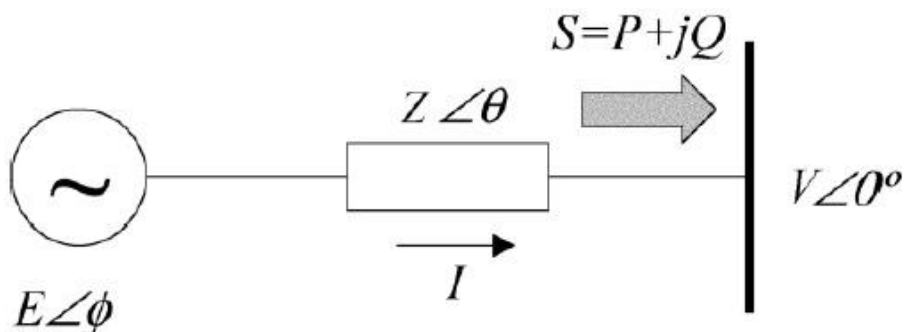
Figure 2.17: The equivalent circuit of a distributed generation unit connected to a common bus

29

In this equivalent circuit, $E < \varphi$ is the inverter open circuit voltage, $V > 0$ common bus voltage, $Z < \theta$ impedance between the inverter and the common bus (sum of inverter output impedance and line impedance), and $S = P + jQ$ is the inverter output power. According to this circuit the inverter output current is as follows:

$$I = \frac{E<\emptyset - V<0}{Z<\theta} = \frac{E}{Z} < (\phi - \theta) - \frac{V}{Z} < (-\theta) \tag{2-10}$$

As a result, the actual and reactive power output of the inverter injected into the shared bus is calculated as follows:

$$P = \frac{V}{Z}[(E\cos\emptyset - V)\cos\theta + E\sin\emptyset \sin\theta] \tag{2-11}$$

$$Q = \frac{V}{Z}[(E\cos\emptyset - V)\sin\theta + E\sin\emptyset \cos\theta]$$

If the impedance Z is a self-propelled Z (Z=X<90), given that φ is a small value, then the (2 - 11) equation is simplified as follows:

$$P = \frac{EV}{X}\sin\phi \approx \frac{EV}{X}\phi \tag{2-12}$$

$$Q = \frac{EV\cos\phi - V^2}{X} \approx \frac{V}{X}(E - V)$$

This relationship shows that with the above assumptions, the real power is more dependent on the phase difference between the inverter voltage and the shared bus and reactive power are more dependent on the voltage range. Therefore, it is possible to control the actual output power of the inverter output voltage phase and control the reactive power output of the inverter output voltage range. Since the phase is a frequency integral, the voltage phase can be indirectly changed by changing its frequency.

In the Droop method, the reference frequency and amplitude of the output voltage of each unit are determined as follows:

$$f = f_n - m_p P \tag{2-13}$$

$$E = E_n - m_q Q$$

Where f_n and E_n are the load frequency and rated voltage output voltage. m_p and m_q, called droop coefficients, are determined by the inverse of the power capacity of each unit.

$$m_p = \frac{\Delta \omega_{max}}{P_{max}} \tag{2-14}$$

$$m_q = \frac{\Delta E_{max}}{Q_{max}}$$

By the above method, assuming that f_n and E_n are the same in all units, in steady state the following relation exists between the output power of the units:

$$m_{p1}P_1 = m_{p2}P_2 = \cdots$$

$$m_{q1}Q_1 = m_{q2}Q_2 = \cdots \tag{2-15}$$

$$P_1 + P_2 + \cdots = P_{Load}$$

$$Q_1 + Q_2 + \cdots = Q_{Load}$$

As a result, the output power of each unit is proportional to its capacity. Assuming the units are the same, the output power of the units will be the same and the load power will be distributed equally between the units. It should be noted that due to the use of a low pass filter in the output power calculation, the droop control bandwidth is much less than the voltage control loop bandwidth and it can be assumed that the voltage control loop can quickly follow the voltage reference specified by the droop control.

2.3.4 General modes of micro-grid performance in the proposed method

In different load conditions, the maximum available PV power and the charge capacity of the micro-grid batteries, the grid can operate in three general modes. In the next section, the performance status of each microcontroller unit is divided into six states, each of which (with the exception of the intermediate state 2,3 which may correspond to the second or third state) corresponds to one of the general states of the microcontroller operation.

It should be noted that, as will be explained, the positioning of the Micro-grid units is decentralized and based solely on local measurements and does not require the information of other Micro-grid units and the amount of Micro-grid load. it also determines the state of the network. Given that the aim of the proposed power management approach is Active power management, reactive power is divided by the common Q-E drop method (Relation (2-13)).

To execute decentralized real power management, the following droop general function is used, which is a modified form of the common droop method:

$$f = f_n + \left(m_p + \frac{m_i}{s}\right)\left(P_{ref} - P_{out}\right) \tag{2-16}$$

Depending on the mode of operation, the coefficients m_p, m_i and f_n and P_{ref} are determined, where f_n is the reference frequency.

State 1:

In this case, the micro-grid load power is greater than the total micro-grid PV power and the batteries provide overload:

$$P_{Load} > \sum_{i=1}^{m} P_{PV-MP_i} \tag{2-17}$$

In this respect P_{PV-MP} is the maximum PV power of unit i depending on the environmental conditions and the amount of sunlight. Three methods can be used to split the overload between batteries:

In the first method, the power load is divided between units according to the common Droop method[1] The values of the relationship coefficients (16-2) for this method are:

$$f_n = f_0, m_p = \frac{\Delta f_{max}}{P_{out-max}}, m_i = 0, P_{ref} = 0 \tag{2-18}$$

Where $P_{out-max}$ is the maximum capacity of the unit inverter and f_0 is the nominal frequency of the micro-grid. In this method, regardless of P_{PV-MP} units, the power is divided solely based on the inverter capacity of the units. The advantage of this method is the balanced distribution of power losses between units, but this method requires the reduction of *PV* power in units with larger *PV* power. As a result, maximum *PV* power is not used.

In the second method, the *PV* incremental converter of all units is controlled so that all solar arrays are produced at their maximum power point $P_{PV} = P_{PV-MP}$). Charging power is divided between units so that the total discharge capacity of the battery needed to supply the overload is divided by capacity and **SoC** of the batteries.

---

[1] Conventional Droop Method

The values of the relation (2-16) coefficients for this method are:

$$f_n = f_0, m_p = m_{pd0} \frac{1}{SoC}, m_i = 0, P_{ref} = P_{PV} \tag{2-19}$$

Where m_{pd0} is a constant coefficient that is chosen in proportion to the capacity of the battery or unit capacity, ie, the battery that has the greater capacity, the m_{pd0} is chosen less to allow greater discharge. This coefficient is also chosen so that the system is stable within the permissible SoC range of each unit and n determines the SoC balancing rate [61].

By $MPPT$, method the PV power is controlled at the maximum power point and the battery per unit maintains the power balance at the dc link, in other words, it provides the difference between the inverter output power and the PV power. Regardless of casualties, the battery charge per unit is as follows:

$$P_{Bat} = P_{out} - P_{PV} \tag{2-20}$$

Therefore (2 - 16) is written as follows:

$$f = f_0 - m_p P_{Bat} \tag{2-21}$$

This relationship, which is similar to the current Droop relationship, results to the division of battery capacity between the units based on their capacity and SoC, so that the unit that has more SoC and capacity, will have more discharge capacity, in order that all batteries will eventually have the same SoC. In this case, the discharge capacity of the batteries will be proportional to their capacity. It should be noted that the battery power is considered positive in the discharge state and negative in the charge state.

In the third method, depending on the capacity and SoC of the battery, the residual capacity of the inverter when the PV is operating at the maximum power point $MPPT$, also plays a part in the load power distribution. In this way, if the capacity and SoC of the batteries are the same, the unit with maximum inverter capacity and P_{PV-MP} will have higher output power. The values of the relationship coefficients (16-2) for this method are:

$$f_n = f_0, m_p = m_{pd0} \frac{1}{SoC} \times \frac{P_{out-max}}{P_{out-max} - P_{PV-MP}}, m_i = 0, P_{ref} = P_{PV-MP} \tag{2-22}$$

In this method, on the first method all units work at maximum power point and the output power of the units is more balanced than on the second method.

The choice of control method depends on the objectives of the micro-grid control. The second method is chosen in this thesis. In this method, in some units, the output power specified by (19-2) may exceed the maximum permitted inverter power of that unit (Condition 5). In this case, the unit is controlled by power (PCM) as follows:

$$m_p = K_{P-P}, m_i = K_{P-I}, P_{ref} = P_{out-max} \tag{2-23}$$

In some units, the unit battery may also be disconnected due to full discharge (situation 4), to prevent damage, in this case the output power is determined by the relation (2-16) with the following coefficients:

$$m_p = K_{P-P}, m_i = K_{P-I}, P_{ref} = \left(K_{V-P} + \frac{K_{V-I}}{s}\right)(V_{dc} - V_{dc}^*) \tag{2-24}$$

Thus, in steady state, the output power of the dc link will be equal to the PV power to maintain the equilibrium of the output dc link. To prevent rapid frequency change and soft state change, f_n is placed in the last two equations equal to the last frequency of the previous unit state.

So, if the micro-grid is in the first state, all units are in either 1, 4, or 5 state.

state two:

In this case, the micro-grid load power is lower than the total micro-grid PV power, but the batteries have the capacity to absorb the excess power. Therefore, all PVs work at maximum power point and the batteries are charged with overcapacity. Due to the maximum allowed power of the batteries, some batteries may be in a limited charge state.

In units that are not in the charge limit state, the inverter is controlled by a voltage control (VCM) and the output power is determined by a relation (2-16) with the following coefficients:

$$f_n = f_0, m_p = m_{pc0}SoC^n, m_i = 0, P_{ref} = P_{PV} \tag{2-25}$$

Where m_{pc0} is selected in proportion to the battery capacity image and the drop coefficient is proportional to the power of the SoC battery. By this method, the battery that has more capacity or less SoC will absorb more power and eventually the batteries SoC will be balanced.

In units with a charge limit state (intermediate status 23), the inverter is controlled by a power control (PCM) and the output power is determined by the interface (2-16) with the following coefficients:

$$m_p = K_{P-P}, m_i = K_{P-I}, P_{ref} = P_{PV} - |P_{ChLimit}| \qquad (2\text{-}26)$$

Where $P_{ChLimit} < 0$ is the maximum allowable battery charge depending on the capacity, voltage, and charge state of the battery and is determined by the method shown in Figure (2-11). In this case, by activating the integral coefficient in relation (2-16), the output power of the unit follows the reference value. By using this method, the battery power is indirectly controlled to the maximum allowable charge because, by avoiding losses, we will have a steady state:

$$P_{bat} = P_{out} - P_{PV} = P_{ChLimit} \qquad (2\text{-}27)$$

In units where there is no battery, the output power is determined by (2-24).

To prevent the frequency change and soft state change, f_n is placed in the last two equations equal to the last frequency of the previous state of the unit.

So, if the micro-grid is in the second state, all units are in either 2 or 23 status.

State three:

In this case, the total charge power and battery charge is less than the maximum power PV of the units. In other words, batteries do not have the full absorption capacity of overcapacity.

$$P_{Load} + \sum_{i=1}^{m} P_{ChLimit_i} < \sum_{i=1}^{m} P_{PV-MP_i} \qquad (2\text{-}28)$$

Therefore, in order to maintain power balance, some units must reduce output PV. In this case, all the batteries are charged at maximum power, some of the units described below will operate at maximum power, and their inverters will be controlled PCM, and their output power will be determined by (2-26) relation., (Intermediate situation 23) Other units reduce the output power and their inverters are controlled VCM and their output power is determined by relation (2-16) with the following coefficients

(Status 3):

$$f_n = f_{max} \, , m_p = \frac{\Delta f_{max}}{P_{out-max}} \, , m_i = 0 \, , P_{ref} = 0 \qquad (2\text{-}29)$$

In units, the voltage V_{dc} is controlled by the incremental PV Converter.

So, if the micro-grid is in the third state, all units are in either 3 or 23 status.

2.3.5 The performance status of each micro-grid unit in the proposed method

In the previous section, the general modes of micro-grid performance are described. In this section, the performance status of each micro-grid unit and switching conditions are described.

Any unit in a micro-grid can operate in one of the following situations:

1. Maximum power of PV and battery discharging

2. Maximum power of PV and battery charging

3. Maximum power of PV and battery charge limitation

4. Reducing power of PV and limit battery charge

5. Maximum power of PV and battery disconnecting

6. Maximum power of PV And output power limitation

Table (2-2) summarizes the performance status of the unit and how the different parts of the unit control each situation.

Situation 1:

This situation corresponds to the first state of the overall performance of the microcontroller. In this situation, the inverter frequency is set by (2-19) and the PV operates at the maximum power point. Battery adapter controls voltage V_{dc} by discharging the battery.

When any of the following conditions is met, the unit exits status 1:

- Whenever the battery power becomes negative (goes into charge mode), the unit goes to status 2.

- When the SoC of the battery reaches its minimum value SoC_{min} (battery drain), the unit goes to state 4.

- Whenever the output power of the unit reaches the maximum value $P_{out-max}$, the unit returns to status 5.

Situation 2:

This situation corresponds to the latter case of the overall performance of the micro-grid. In this situation, the inverter frequency is set by (2-25) and PV operates at the maximum power point. Battery adapter Controls voltage V_{dc} by charging the battery.

When any of the following conditions is met, the unit exits status 2:

- When the battery power is positive (Enter discharge mode) the unit goes to status 1.

- Whenever the charge current, charge power, or voltage of the battery reaches its maximum value (the battery reaches the charge limit), the unit goes to status 23.

Situation 23:

This is a transitional state between states 2 and 3. This state is shared between the second and third modes of the entire micro-grid, where the inverter is controlled by PCM. The unit enters the state when the battery reaches the limit of charge in status 2 or reaches the maximum PV power point in status 3. In this case, the PV operates at the maximum power point and the battery-voltage adapter V_{dc} converts to controls the battery charge. By controlling the output power by (2-26), the battery is indirectly controlled in the charge limit state.

Exiting the state 23 is as follows:

- By reducing the load power, increasing the total PV power output, or reducing the battery charge of the micro-grid units that are in the 23rd position, the battery charge of the units in the 2nd state increases, and all units changes from state 2, to this state one after another. After switching all units to $state$ 23, due to the integration function in the relationship (26-2) and due to the lower load power than the reference power, the frequency f gradually increases to be saturated to its maximum value f_{max}. At this point, all units are shifting to $status$ 3 to

reduce the total *PV* production capacity and maintain the balance between production and consumption.

- When the micro-grid is in the second state (all units are in *status* 2 or *state* 23), any increase in load power or a decrease in *PV* power reduces the overall battery charge. In this case because of the battery charge of the units that are in the 23 *state* remains constant at its maximum value, only the charge of the units in *condition* 2 decreases, and the unbalance between the units of the battery increases. To ensure a balanced distribution of power between batteries (depending on capacity and *SoC*), whenever for any of the units which are in *status* 23, Battery-powered charge of that unit exceeds the battery-powered charge of units in *status* 2, that unit must return to *status* 2:

$$m_{p-i}|P_{Bat-S2-i}| < K_{pm}m_p|P_{Bat}| \tag{2-30}$$

In this relation, P_{Bat} unit battery power, $P_{Bat-S2-i}$ unit battery charge of i, which is in *state* 2, and $K_{pm} < 1$ is a factor to prevent unwanted state change due to errors in measuring battery power. It is noteworthy that according to (2-21), since the total frequency of the micro-grid is the same, $m_{p-i}P_{Bat-S2-i}$ is equal to all units in *status* 2.

Given that P_{Bat} is in negative charge mode, (2-30) is written as follows:

$$m_{p-i}P_{Bat-S2-i} > K_{pm}P_{Bat} \tag{2-31}$$

Using (2-20), (2-25) and (2-31), The condition for return to *status* 2 is as follows:

$$f < f_0 - K_{pm}m_pP_{Bat} \ and \ 2 =$$
$$previous \ state \tag{2-32}$$

That is, when the unit frequency is lower than the calculated value in this respect and the previous state of the unit was *state* 2, if the unit returns to *status* 2 and its charging capacity is set to (2-25), the unit will not return to the charging limit state again. In the special case where the unit is in the *state* 23, and the battery charge is zero due to the battery being fully charged, whenever $f < f_0$ it indicates that the other units are in the discharge state and

consequently this unit also switches to the *state* 2 and it contributes to the power supply by charging the battery.

- By increasing the power of the micro-grid or decreasing the generating power of the *PV* unit, which results in increasing of the total charge of the battery and the output power of each unit relative to its *PV* power, all units switch one after another from *state* 3 to this state. In this case, because of the integration function in the relation (2-26) and due to higher output power than the reference power, the frequency f is gradually reduced to reach f_0. At this time, all units are switched to *status* 2 to maintain a balance between production and consumption by reducing battery power.

- When the micro-grid is in the third state (all units are in *state* 3 or *state* 23), any reduction in charge capacity or total battery charge of the micro-grid units, reduces the total power *PV* required.

- In this case, because the output power of the units in *state* 23 is constant and at the maximum power point, only the PV power of the *state* 3 decreases, causing an unbalanced increase in the load power distribution between the units and the *PV* output of the units. To resolve this problem, whenever for each of the units in *state* 23 the weighted output power of that unit exceeds the weighted output power of the units in *status* 3, the unit must return to *status* 3

$$m_{p-i}P_{out-S3-i} < K_{pm}m_pP_{out} \tag{2-33}$$

Where P_{out} is the output power of the unit and $P_{out-S3-i}$ the output power of the unit i which is in state 3.

It is worth to mention that in steady state, P_{out} with P_{ref} Designated by (2-27) are equal, and according to (2-29), $m_{P-i}P_{out-S3-i}$ (1) are same for all units in status 3. Using (2-29) and (2-33), the condition of returning all states to state 3 is as follows.

$$f > f_0 - K_{mp}m_pP_{out} \text{ and } 3 = previous\ state \tag{2-34}$$

When this condition is set for frequency and the unit returns to state 3, and its output power is with respect to (2-29) relation, and due to insufficient power of PV will no longer return to $state$ 23.

Situation 3:

This situation corresponds to the third state of the micro-grid where the maximum power of PV units are greater than the total power required to charge the batteries. In this case, the unit battery is charged at the maximum allowed power, the unit output power is determined by (2-29), and the incremental PV adapter controls the voltage V_{dc} and maintains the power balance at the dc link. In this case, the output power PV which is the sum of the battery charge and the output power of the unit, is less than its maximum power.

The condition for exiting state 3 is as follow.

- Whenever increasing the load power or decreasing the PV power of other units increases the output power of the unit

As the total output power and battery charge of the unit exceeds its maximum PV power, the unit switches to $state$ 23. Also, when all units go from $state$ 23 to $state$ 3 but PV power is not enough for this unit, the unit returns to $state$ 23. It should be noted that reaching the PV to the maximum power point is detected by the dc link voltage drops. When the total output power and battery charge of the unit exceeds its maximum PV power, the PV adapter is unable to control V_{dc} voltage and the V_{dc} voltage is reduced and after reaching the minimum allowable voltage, the unit returns to $state$ 23. Also, if in Fig. 2-9 the reference PV voltage reaches the V_{PV-MP}, which has been set since the last $MPPT$ implementation in other situations, then the unit also goes to $state$ 23. If the V_{PV-MP} has changed since its last value, no problem will happen because by changing the state to $state$ 23, this point is re-tracked and if increased to the new point, the condition (2 - 32) is restored and the unit goes back to state 3.

Situation 4:

Whenever the SoC of the unit battery reaches its minimum SoC_{min} limit, the unit goes into this state.

In this situation, the battery will be disconnected to prevent damage due to severe discharge, the PV will operate at maximum power point and the V_{dc} voltage will be controlled by (24-22). Since $P_{Bat} = 0$, in steady state

$$P_{out} = P_{PV-MP} \qquad (2\text{-}35)$$

When all units enter this state and the load power is less than the sum of the maximum power (PV), f decreases until it reaches its critical value.

In this case some non-sensible loads should be cut off (Load Shedding).

Managing the load shedding is not within the scope of this review.

the condition of exiting state 4 is as follows.

- According to (2-21), whenever $f > f_0$ it indicates that the micro-grid has entered the second state and the batteries in the micro-grid are being charged. In this case, the unit can return to $status$ 1 to automatically switch to $status$ 2 and charge the battery.

Situation 5:

Whenever the unit output power reaches its maximum permissible value $P_{out-max}$, it switches to limit the output power. In this state PV operates at the maximum power point and controls the battery voltage adapter V_{dc}. Output power is controlled by (2-23) with $P_{ref} = P_{out-max}$. If all units are in this condition and the load capacity exceeds the total capacity of the units, the frequency is reduced and some non-sensing loads must be cut off.

the condition of exiting state 5 is as follows

- Whenever some units that are in $status$ 1 due to reduced power or increased PV power of the battery, the units that are in $status$ 1 of the unit will be less than the power of this unit's weight, this unit can return to $status$ 1.

$$P_{P-i}P_{Bas-S1-i} < K_{pm}m_pP_{Bat} \qquad (2\text{-}36)$$

According to (2-21) this condition can be written as follow.

$$f > f_0 - K_{pm}m_pP_{Bat} \qquad (2\text{-}37)$$

Whenever this condition is set for frequency and the unit returns to $state\ 1$, the output power of the unit will be less than $P_{out-max}$ and the unit will not return to $state\ 5$.

The various conditions for changing the status of each unit in the subnet are summarized in Figure (2-7).

It is worth to mention that in the proposed method, there is no need to measure network frequency for use in switching conditions. This is because when the inverter is controlled as VCM, like the common droop method, all units reach a common frequency in steady state [62]. also, when the inverter is controlled as PCM, it follows the grid frequency due to the integration function in controlling the output power. For this reason, the unit frequency can be used as f in the above conditions and does not require precise measurement of the network frequency. However, when setting up and connecting the unit to the micro-grid, the output voltage of the unit must be synchronized with the micro-grid voltage, which will result in the unit frequency being equal to the micro-grid frequency.

Figure (2-19) shows the characteristic $P - f$ of a micro-grid consisting of two hybrid units in different positions.

In $Fig.A$ both units are in $state\ 1\ or\ 2$. The units shown in the figure have the maximum power PV and are assumed $SoC_1 > SoC_2$. The fI frequency is a typical working frequency at a specified load power in which the micro-grid operates in the Situation 1 and the units are in state 1. Due to the difference in the characteristic slope $p - f$ of the two units, the output power of the units at this $P_{outI}1\ and\ P_{outI}2$ frequency is such that $unit\ 1$ discharge power is greater than $unit\ 2$ discharge power $P_{Bat-Dis}1 > P_{Bat-Dis}2$. When the load power is lower than the total power PV, the micro-grid enters the $second\ state$. The frequency f_{II} shown in the figure is a typical working frequency at a specified load power in which the micro-grid operates in the $situation\ 2$ and the units are in $state\ 2$ and the output power $(P_{outII-1}\ and\ P_{outII-2})$ at this frequency is such that Charging $unit\ 1$ is less than charging $unit\ 2$ $(|P_{Bat-Ch1}| < |P_{Bat-Ch2}|)$. As the load decreases further, the unit's charge power increases. Assuming $unit\ charge\ 2$ is greater than $unit\ 1$ $(|P_{ChLimit1}| < |P_{ChLimit2}|)$, $unit\ 1$ enters $state\ 23$. The bold lines in $Fig.(B)$ show the condition that $unit\ 2$ is in position

1 and $unit$ 1 is in position 23. The output power of $unit$ 2 is controlled by the value $P_{PV-MP} + P_{ChLimit1}$ and the $unit$ 2 supplies the remaining load power. In addition, $Unit$ 1 follows the frequency set by $Unit$ 2. Note that the $f_{S2\to1}$ frequency is the frequency at which $unit$ 1 can return to $state$ 1 when load power is increased. This frequency is equal to the condition (2 - 32) with respect to $K_{pm} = 1$ On the other hand, when the batteries are discharged, the output power of both units increases. Because $Unit$ 2 has larger P_{PV-MP} power, it reaches the output power limit earlier than $Unit$ 1 and switches to $state$ 5 and controls output power at $P_{out-max}$.

Bold lines in $Fig.(c)$ show where $unit$ 1 is in position 1 and $unit$ 2 is in position 5. The frequency $f_{S5\to1}$ with condition (2-37) and with the respect $K_{pm} = 1$ are equal, Is the frequency at which $unit$ 2 can return to $state$ 1 when the load power is reduced. When PV power is available from the sum of the load power and charge of the micro-grid batteries

Increasingly, the micro-grid operates in the $third\ state$. $Fig.(d)$ shows the state where both units are in $state$ 3. Frequency f_{III} is a typical working frequency in which both units have the same output power due to the same of m_p. As load power increases, $Unit$ 1 reaches its maximum PV power and changes to $state$ 23. Bold lines in $fig.(e)$ characterize two units when $unit$ 1 is in $state$ 23 and $unit$ 2 is in $state$ 3. The frequency $f_{S2\to3}$ with condition (2-34) and with the respect $K_{pm} = 1$ are equal, Is the frequency at which $unit$ 1 can return to $state$ 3 when the load power is reduced.
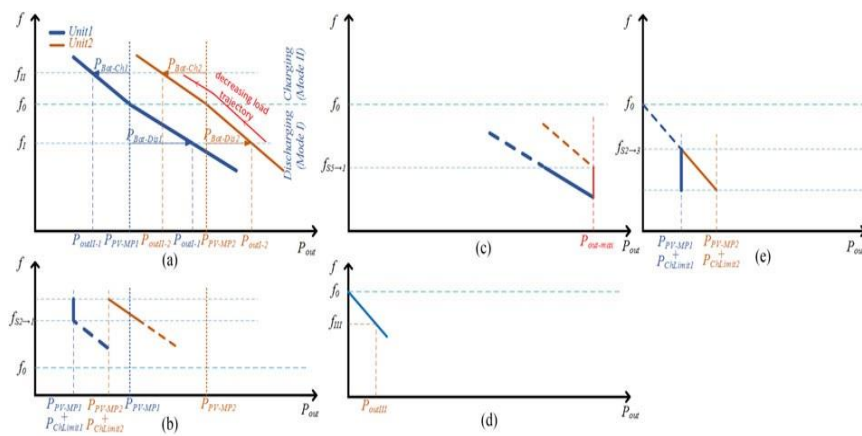
Figure 2.18: Characteristic $p - f$ a microgrid composed of two different hybrid status
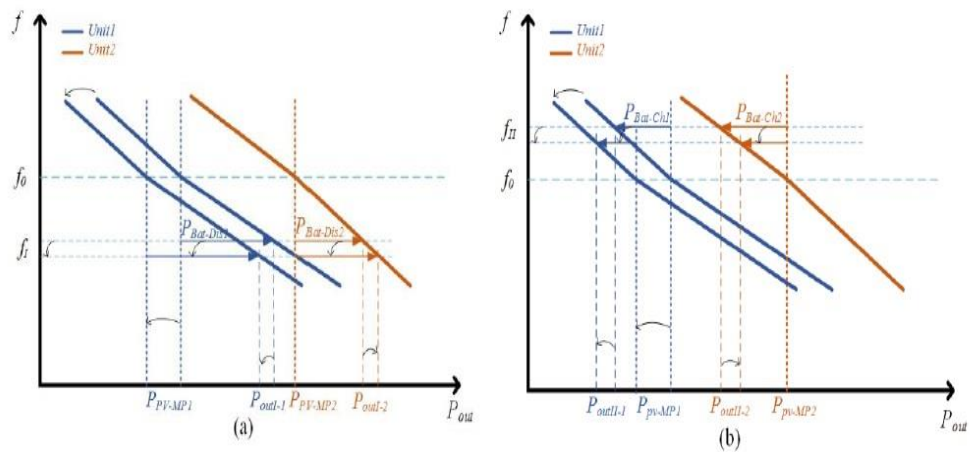
Figure 2.19: Characteristic displacement $p - f$ and working point due to decrease in maximum PV power of $unit$ 1

a) First situation

b) Second situation

$Figure$ $(2 - 20)$ shows the displacement of the characteristic $\boldsymbol{p - f}$ and the working point due to the reduction of the maximum power PV of $unit$ 1 while the load power is kept constant.

By decreasing in P_{PV-MP1} attribute $p - f$ of $unit$ 1 is moved to the left. $Fig.(A)$ corresponds to the operating frequency f_I in (2-19 a). Due to the decrease in PV power, the discharge power of both units increases. The output power of unit 1 also decreases and the output power of unit 2 increases. Fig. (b) corresponds to the operating frequency f_{II} in Figure (2 - 19a). due to the reduction in PV power, the charging power of both units is reduced. The output power of $unit$ 1 also decreases and the output power of $unit$ 2 increases.

3. DECENTRALIZED POWER MANAGEMENT IN SINGLE PHASE / THREE PHASE HYBRID MICROGRID

3.1 Introduction

In the last chapter, a method for decentralized power management in single-phase micro-sources with a combination of solar and battery sources was presented. In this chapter, the proposed method is extended to single-phase / three-phase hybrid micro-networks including stand-alone, hybrid PV units and battery units like micro-grid shown in figure (3-1).
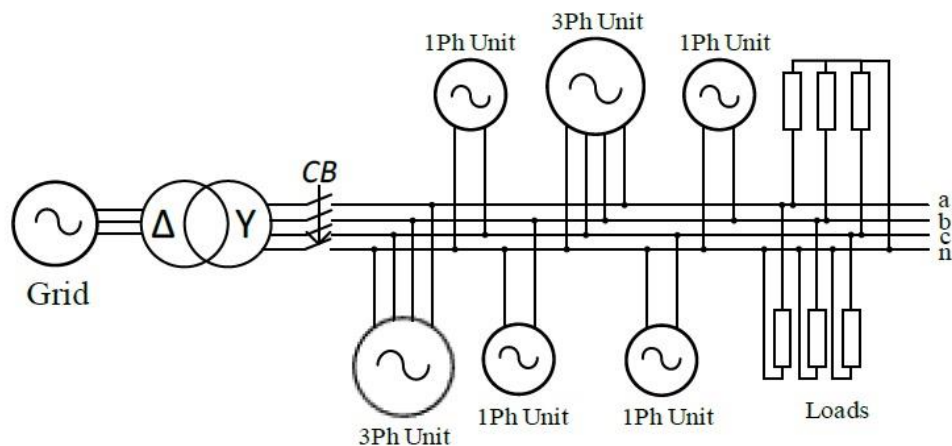
Figure 3.1: Single Phase / Three Phase Hybrid Network

It consists of single-phase and three-phase units connected to a four-wire three-phase system. Single phase units are connected to different phases and there can be several single-phase units in each phase. This micro-grid is connected to the main grid by a *ΔY* transformer and a circuit breaker key. When an error occurs on the main grid, the key is disconnected, and the grid continues to operate in a separate or (islanded) state from the grid. In this thesis, only the state of the grid of this micro-grid is examined. The input source for single phase and three phase units can be PV, battery or combination of PV and battery. For the sake of simplicity of results and analysis, this micro-grid monograph is shown in Figure (3-2).
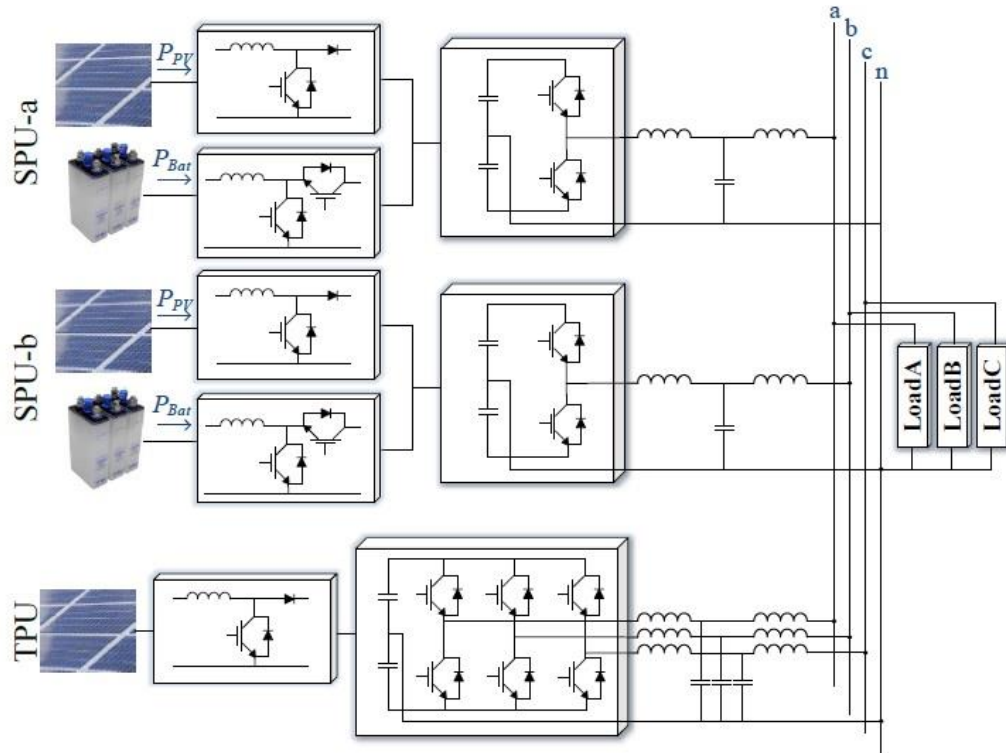
Figure 3.2: The single-phase / three-phase hybrid micro-grid considered in this thesis

It consists of a three-phase unit with a PV input source, mentioned as TPU, and two single-phase units with a combined source connected to phases **a** and **b**, called SPU-a and SPU-b, respectively. No single-phase unit is connected to phase **c**. All micro-grid loads are concentrated in three single-phase loads connected to different phases. Single-phase units from a single-phase half-bridge inverter connected by an LCL filter to a common PCC junction, a PV array connected to a dc link by a one-way adapter and a battery by a two-way adapter Linked to dc link, composed. The three-phase unit consists of a four-wire, three-phase inverter that is connected to the PCC by the LCL filter and a PV array that is connected to the dc link by a one-way incremental converter.

The method presented in this dissertation has the following characteristics, without the need for any link between units and without knowing the amount of charge in each phase.

- Power management is possible in all single-phase and three-phase hybrid micro-networks consisting of PV, battery and hybrid units.

46

- When the sum of the micro-grid load exceeds the sum of the maximum PV units, all PV sources available in micro-grid (in single phase or three phase units, standalone or hybrid) works at maximum power point (MPP) and all batteries in micro-grid (in single phase or three phase units, Standalone or combined) provide overload power. Also, overload power is being sheared between batteries the battery with a higher SoC has a higher discharge level, until the SoC in Batteries are balanced.

- When the maximum PV power of the unit exceeds the total charge of the micro-grid, but the batteries are available

In the micro-grid, they have the capacity to absorb the excess PV power, the batteries are charged by the PV excess power Split the charge between batteries so that the less SoC, the more charge

- So that the SoC of the batteries will eventually balance. The division of power between the battery charging SoC of battery is such that less can be more charged So that the SoC of batteries will eventually balance.

- When the total PV power of the unit exceeds the total charge of the micro-grid and the batteries in the micro-grid reach their maximum SoC or maximum charge, the power output of some PV units is getting lower than the MPP point in order to balance the production and consumption.

- In all cases, the limitations of the SoC and the maximum battery charge as well as the capacity of the inverters are considered.

- Power transfer between different phases is done automatically through three-phase units so that the loads in one phase can be fed through the PV power or battery of the other phases or the batteries can be charged from the power of the other phases.

3.2 Decentralized Active Power Management In Micro-Grid

The general method of power management in the single phase / three phase hybrid micro-grid and the overall block diagram of each unit are similar to the method presented in Chapter 2. The block diagram of the inverter control section of each three-phase unit is shown in Figure 3-3. In this form, to

calculate the inverter output power, the active and reactive power of the main component of the voltage and current in each phase is calculated and the total power of the inverter is calculated from their sum. The control method for single phase units is similar to the previous chapter. Since the purpose of this thesis is to present a new method for active power management, reactive power sharing is performed using the methods presented in previous researches. Therefore, it is possible to choose the appropriate method according to the objectives of the micro-grid. In this thesis, the reactive power division is performed separately in each phase so that the reactive power in each phase is divided according to the droop coefficients between the single-phase units and the corresponding phase units of the three phase units. In this method, three-phase units are considered as single-phase units in terms of reactive power. One of the disadvantages of this reactive power division is the high voltage imbalance in the output of the three phase units. For example, if in one three-phase unit, the reactive power of one phase is positive and the reactive power of the other phase is negative, the output voltage difference of those two phases will increase. If there is a load imbalance sensitive to the micro-grid, a low bandwidth telecommunication link and the method presented in [63] can reduce the voltage imbalance to the desired level.
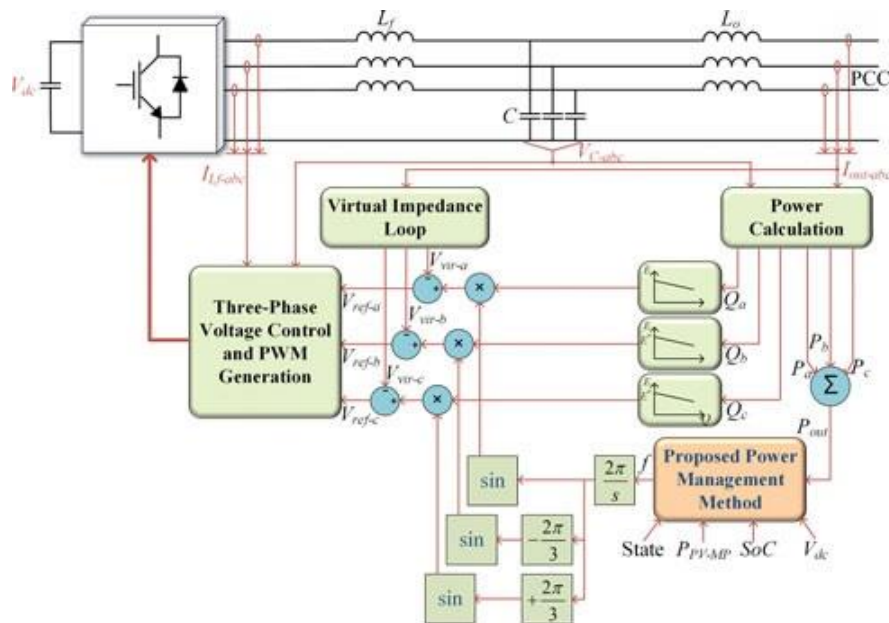
Figure 3.3: Inverter control diagram of three phase units

3.2.1 General modes of micro-grid operation and operating status of each micro-grid unit

Similar to single-phase micro-grid, hybrid micro-grid can also be described in three general modes described in previous Chapter.

In first case the micro-grid load power is greater than the total micro-grid PV power and the batteries provide overload power, and this overload power is divided between the batteries by the general Droop function **(2-16)** with coefficients **(2-19)** which is repeated for simplicity.

$$f = f_0 + \left(m_p + \frac{m_i}{s}\right)\left(p_{ref} - p_{out}\right) \qquad (1\text{-}3)$$

$$m_p = m_{pd0}\frac{1}{SOC^n} \, , \, m_i = 0 \, , P_{ref} = P_{PV-MP} \qquad (2\text{-}3)$$

In second case, the micro-grid load power is lower than the total micro-grid PV power, but the batteries have the capacity to absorb the excess output. Therefore, all PVs work at maximum power point and the batteries are charged with overcapacity. The units in the **VCM** mode are controlled by the coefficients **(2-25)** and the units in the PCM state are controlled by the coefficients **(2-26)**, which are repeated below.

$$m_p = m_{pc0}SoC^n \, , m_i = 0 \, , P_{ref} = P_{PV-MP} \qquad (3\text{-}3)$$

In the *situation* 3, the total charge and charge capacity of the batteries are less than the maximum (PV) power of the units, in other words, the batteries do not have the full absorption capacity of the generating power, so to maintain power balance, Some PV units have to reduce their production. Units that are in VCM are controlled by the coefficients (2-29):

$$m_p = \frac{\Delta f_{max}}{P_{out-max}} \, , m_i = 0 \, , P_{ref} = 0 \qquad (3\text{-}4)$$

It should be borne in mind that in the proposed method, there is no need to know the load rate of each micro-grid phase.

The performance status of single-phase units is like the previous season. Each three-phase unit in the grid, in addition to the six single-phase units, can operate in the following two situations:

- 5a- One Phase Output Power Limit

- 5b- One-Phase Output Power Limit and Charging Limit

Table (1-3) Summarizes The Performance Status Of The Three-Phase Units And How The Different Parts Of The Unit Control Each Situation.

Table 1.3: Summarizes The Different States Of A Three-Phase Micro-Grid Unit

Situations	1	2	23	3	4	5	5a	5b
Explanation	Maximum **PV** power and Battery discharge	Maximum **PV** power and Battery charge	Maximum **PV** power and Battery charge limit	Reduced **PV** power and limited battery charge	Maximum **PV** power and Battery Disconnect	Maximum **PV** power and output power limit	Maximum **PV** power and single-phase output power limit	Maximum **PV** power and one-phase output power limit and battery charge limit
Inverter control type	Voltage control (2-19)	Voltage control (2-25)	Power control (2-26)	Voltage control (2-29)	Power control (2-24)	Power control (2-23)	Power control (3-5)	Power control (3-5)
Battery control type	Control of V_{dc}	Control of V_{dc}	Control of V_{dc}	Charge limit	Disconnect	Control of V_{dc}	Control of V_{dc}	Charge limit
PV control type	Maximum power	Maximum power	Maximum power	Control of V_{dc}	Maximum power	Maximum power	Maximum power	Control of V_{dc}
Corresponding Micro-grid Mode	First	Second	2nd / 3ird	Third	First	First		

Situations 1 through 5 are the same as those described in the previous chapter.

situations 5-A and 5-B will be explained.

Situations 5-A and 5-B:

As will be explained below, in a single-phase power unit the different phases may have different directions (positive or negative). Therefore, although the total power of the unit is less than the maximum value, $P_{out-max}$, the output power of one phase may reach the maximum phase power, PI.

$$P_{ref} = P_{out-max} + \left(K_p + \frac{K_i}{s}\right)\left(P_{phase-max} - P_{phase-x}\right) \qquad (3-5)$$

This can happen in any of the 1, 2 or 23 situations. In Fig. 5a, the battery is in a charge limit state and can absorb excess power of (PV) while the output power is reduced to less than P_{PV-MP}. In this state (PV) it operates at maximum power and controls the battery voltage adapter V_{dc}.

In the 5b state, the battery is in the charge limit state and the PV power is reduced to less than P_{PV-MP}. In this case, the PV converter controls the V_{dc} voltage.

Exiting the condition 5a is as follows:

- Same as situation 5 if the condition (2-37) is fulfilled the unit return to state 1.

$$f > f_0 - K_{pm}m_pP_{Bat} \tag{3-6}$$

- When the battery is fully charged and the battery charges or voltage reaches to its maximum voltage, the status changes to status 5B.

Exiting the condition 5b is as follows:

- When the power (PV) reaches its maximum value, the unit returns to state 2.

The various conditions for changing the status of each three-phase unit in the micro-grid are summarized in Fig.
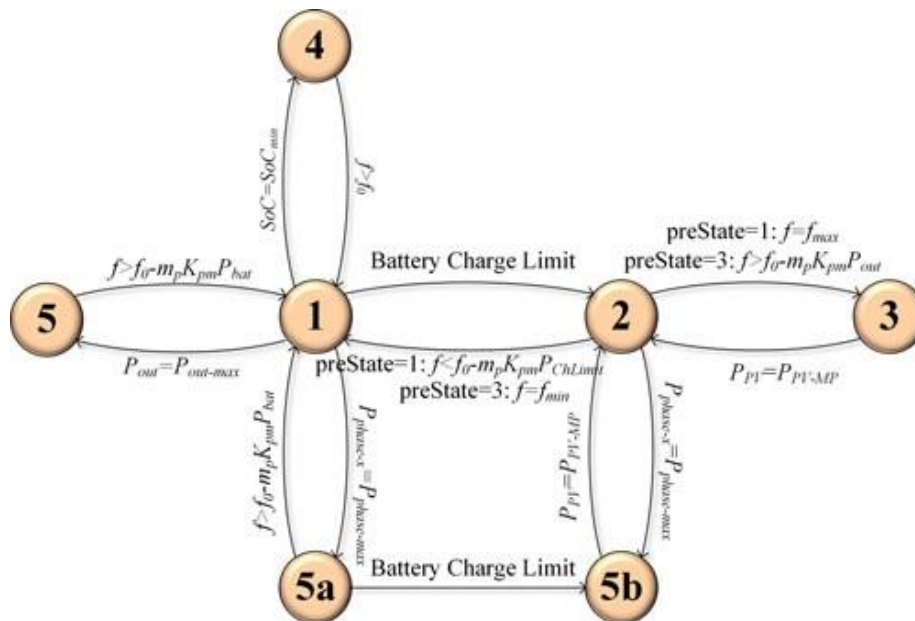
Figure 3.4: Criteria for transition between the states in each unit in the MG.

3.2.2 Power transfer between different phases

For analyzing the automatic power transmission between different phases in the micro-grid, the micro-grid (Figure 3-2) is considered. There can be various conditions in the operation of this micro-network. When all units are in 3 , the output power of the units is determined by (3-4). Since in the steady state, frequency of all units is the same, the following relationships exist between the sum of the outputs of the three-phase unit and the output power of the single-phase units:

$$\left\{ \begin{array}{l} f = f_0 - m_{TPU}P_{TPU} \\ f = f_0 - m_{SPU-a}P_{SPU-a} \\ f = f_0 - m_{SPU-b}P_{SPU-b} \end{array} \right\} m_{TPU}P_{TPU} = m_{SPU-a}P_{SPU-a} = m_{SPU-b}P_{SPU-b} \quad (3\text{-}7)$$

$$P_{TPU} = P_{TPU-a} + P_{TPU-b} + P_{TPU-c}$$

In addition, the equilibrium of power in each microgrid phase leads to the following equations:

$$P_{TPU-a} + P_{SPU-a} = P_{LD-a} \; ; \quad P_{TPU-b} + P_{SPU-b} = P_{LD-b} \; ; \quad P_{TPU-c} = P_{LD-c} \quad (3\text{-}8)$$

Using these equations, the output power of single-phase units and the output power of each three-phase unit are accurately determined. It is worth to mention that P_{TPU-a}, P_{TPU-b} or P_{TPU-c} can be negative, indicating that power is transferred from one phase to another.

In other cases, the same relationships determine the output power of the units. For example, if **SPU-a** is in status (23) and other units are in status (3), then (3-7) is written as follows.

$$\left\{ \begin{array}{l} f = f_0 - m_{TPU}P_{TPU} \\ f = f_0 - m_{SPU-b}P_{SPU-b} \end{array} \right\} => m_{TPU}P_{TPU} = m_{SPU-b}P_{SPU-b}$$
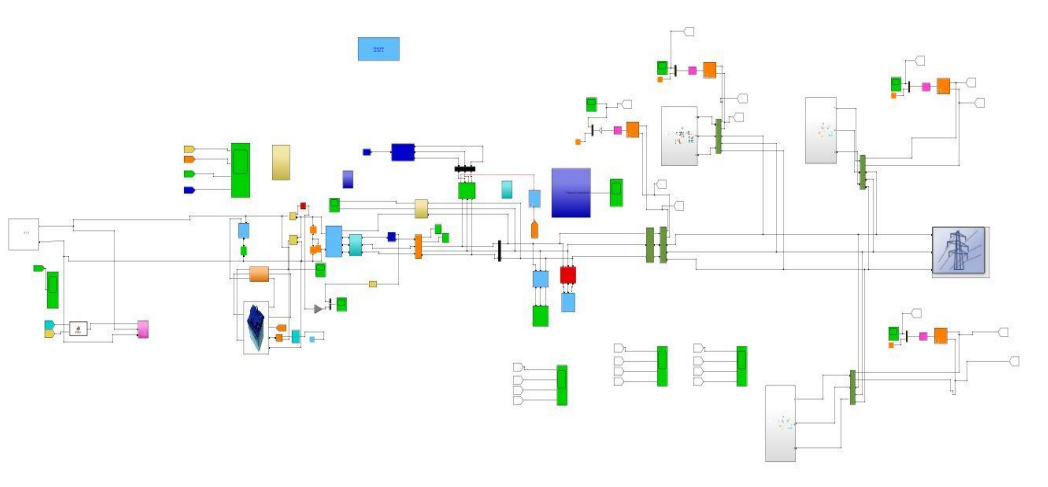
$$P_{SPU-b} = P_{ref-b} \qquad\qquad\qquad\qquad\qquad\qquad (3\text{-}9)$$

$$P_{TPU} = P_{TPU-a} + P_{TPU-b} + P_{TPU-c}$$

4. EXPERIMENTAL RESULTS

4.1 Main Circuit

This chapter will explain the main circuits, and control of each part of the circuits and at the end will be shown each circuit output independently. Below shown figure 4.1 is complete main circuit.

Figure 4.1: subsystem 1 complete layout.

4.2 Proposed Methodology

In this novel we have four DES (distributed energy resources), Each Subsystem connected with the battery for power storing and connected in parallel to each other. Output of each subsystem is converted into AC by inverter. Our aim in this thesis is to obtain three phase power to the load connected with grid, that varies with different load conditions, Each Subsystem has direct connected load, the spare power the shared with the grid and also given to battery to maintain SOC (state of charge) of the battery so that in case of absence of any resource the demand could be feed properly with the help of Battery storage.

Networked Microgrid have four subsystem whose detail are as given below,

- Subsystem 1

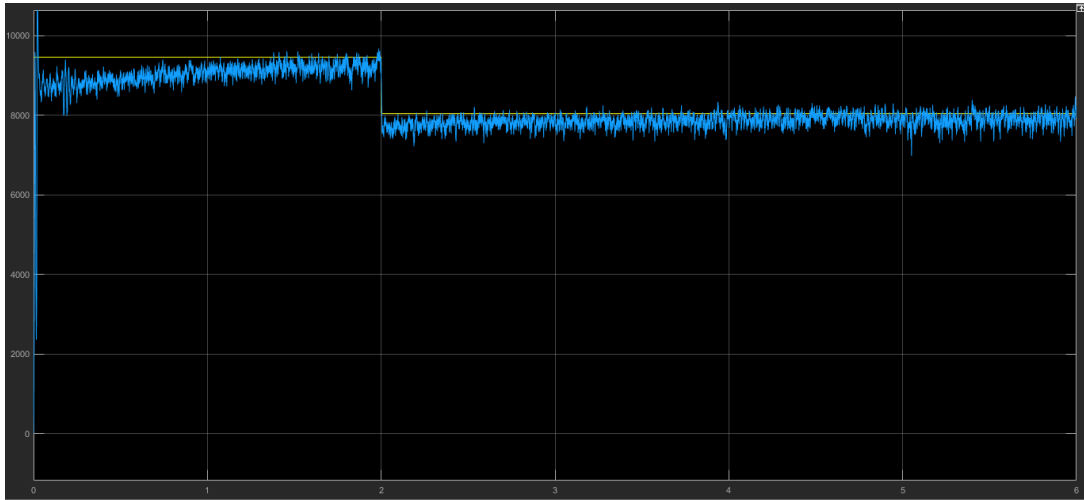- Subsystem 2

- Subsystem 3

- Subsystem 4

All the Systems are system in term of generation the only difference is in the load connected to the systems.

4.3 Working of PV subsystem 1

We have used two solar modules each produces 666 volts and they are connected to each other in parallel, here two values of solar irradiance, one is constant (1000) and other is variable (1000 at zero-time index and 850 at time index 2) are connected as input to solar arrays. A system is installed to track the MPPT output of the solar modules, a free-wheeling diode is used to prevent the system from the reverse currents in order to prevent from system damage.
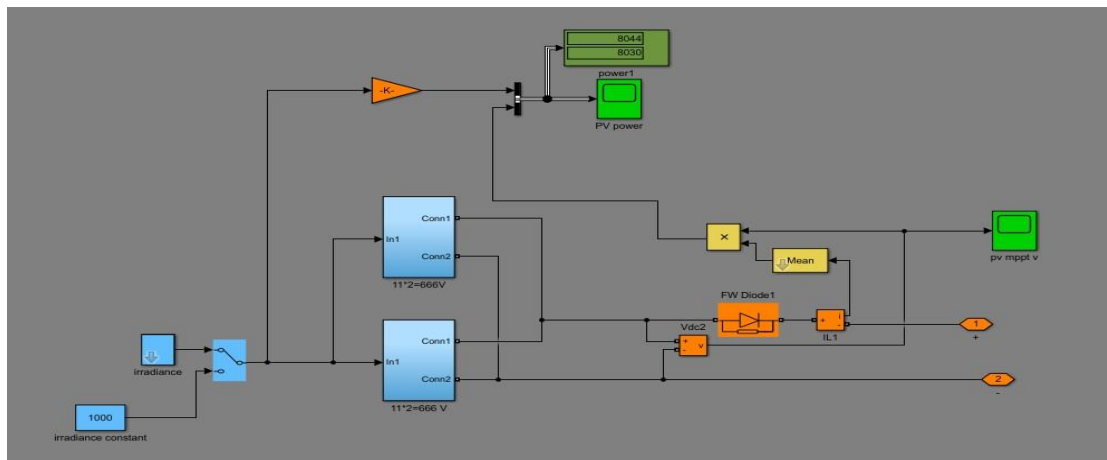
Figure 4.2: Circuit of PV subsystem 1

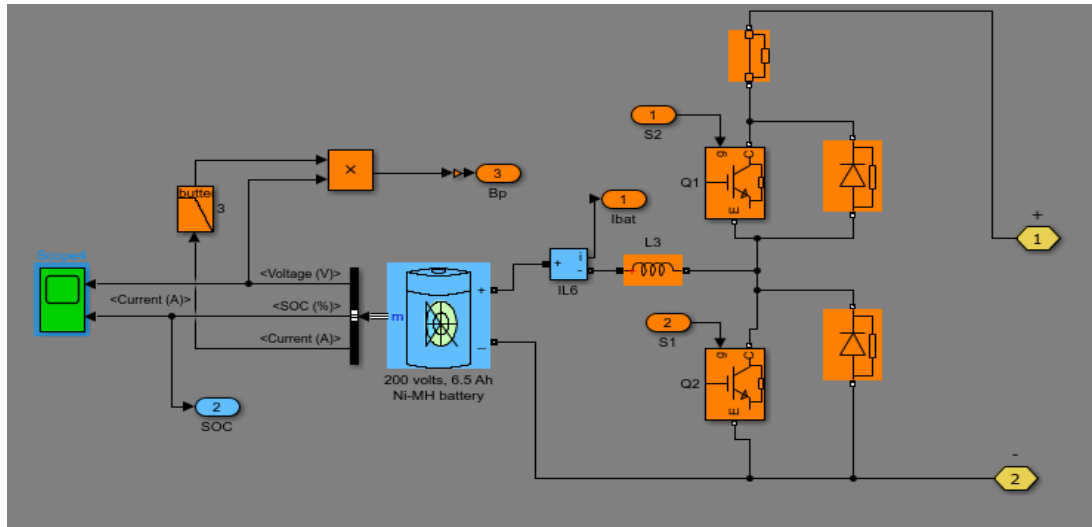**Figure 4.3:** power generated by PV solar panels of subsystem

4.4 Methodology Description

Above pictures gives the stats of the generated power by PV modules, initially there is instability in the system, which is in transients condition, later this become stable in steady state operation. After 2 unit index on the x-axis, there is a little reduction in power due to the variability of the solar irradiance, and hence there is a little less power obtained by the system, the mean value of the power is about 9kw, **there is additional** load is attached to the system which is around 16kW and the Subsystem 1 itself produces approximately 9kw, the extra power is supplied by the battery and the other subsystems because they contains less load so they have the extra energy to share with subsystem 1.

4.5 Operation of Battery System of Subsystem 1

The battery system also known as storage subsystem, is the backup system which is deployed to share the power to the system in case if generation resource is absent or there is extra load connected, so to cope this issue battery system is used as backup. this system is consisted of A battery bank, here we have used the 200 volts 6.5 Ampere hours Ni-MH battery, IGBT's for switching purposes, the battery power, state of charge and voltage monitor system, the battery system controlled by PID controller system (which will be discussed later), if the battery state of charge is below than the permissible limit the conventional method will be requested to supply the energy, so that the load

will get the abrupt supply from the system, and battery will be recharged if there is excess power available on the system. There is an inductor L3 used in series with IGBT and battery for protection purposes.

Figure 4.4: Charging and discharging of Battery System

4.6 Battery voltage and SOC of Subsystem 1 Description

As we can see from the below plot of fig 4.4, the voltage of the battery are around 300Vdc in transient condition, but later with a short span of time the voltage are around the rated 285Vdc in transient condition, Battery SOC is decreasing because there is additional load is attached to the system which is around 16kW and the Subsystem system 1 itself produces approximately 9kw, the extra power is supplied by the batter and the other subsystems because they contains less load so they have the extra energy to share with subsystem 1.
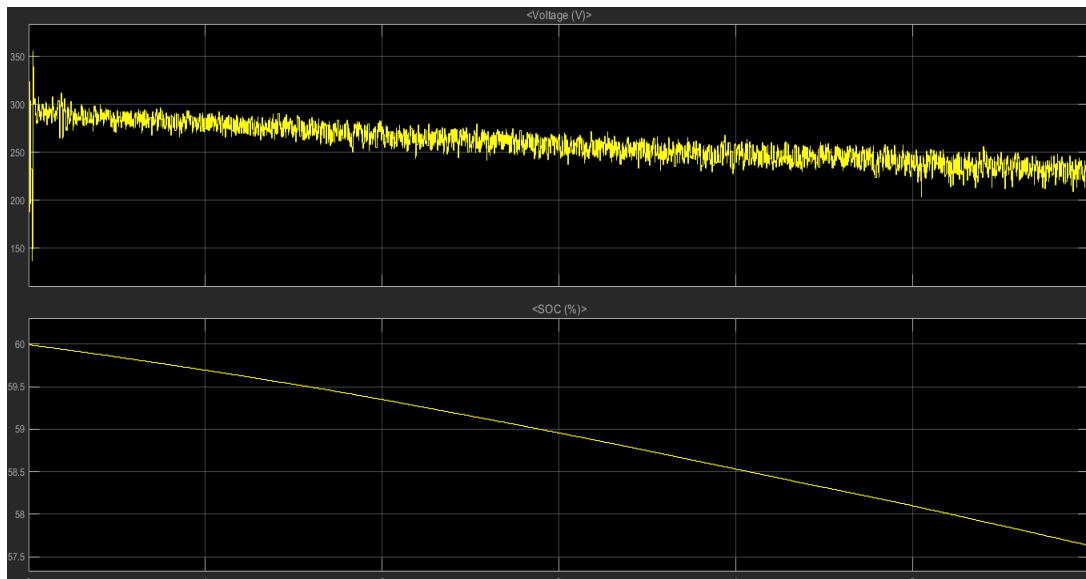
Figure 4.5: Battery voltage and SOC of Subsystem 1

4.7 Operation of PID Controller

This is basic control system for switching process of battery to operate at different time according to the load and other resources.

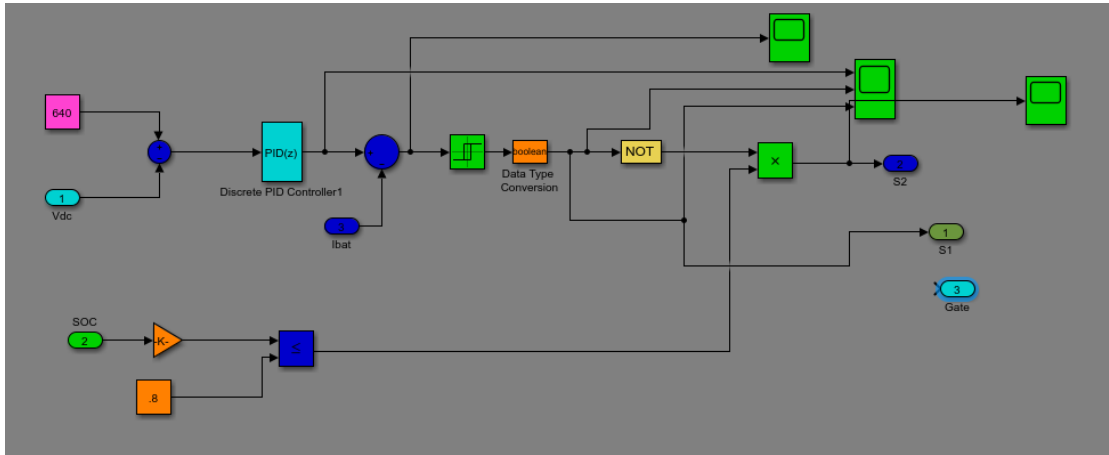Here, two parameters of battery are taken into consideration that are:

- Voltage of battery
- Battery SOC

Initial SOC of battery 85% and response time 30 second that means whenever soc reach to 80%, it indicates that battery is fully charged.

This part is for voltage regulation of the battery this part will decide when voltage to increase and when to drop, whenever it senses load power is not compensated by other resources then it provides pulse to the switches s1 and s2, in this input to the PID is the comparison value of vdc and reference value.

PID works to achieve desired value. It provides switching pulses through s1 and s2 which in input to the MOSFET.

Battery management using SOC control system here input is soc of the current situation, in next step it is compared with some value of soc, that whenever the soc reached its minimum it provides pulses to s1 and s2 for recharging of battery.

57

Figure 4.6: Power Control by PID Controller

4.8 Operation of PWM Inverter

As the circuit shown below, three phase inverter is used to convert the DC power to 3-phase AC with a standard frequency of 50-Hz, we need to remember that the output power of solar system is DC, and the load connected is three phase AC, so we have to convert to 3-phase AC. This system is made of IGBT's, and then this power is filtered with the help of LC filter so the DC components can be removed from the power so that the power quality of the system can be maintained.
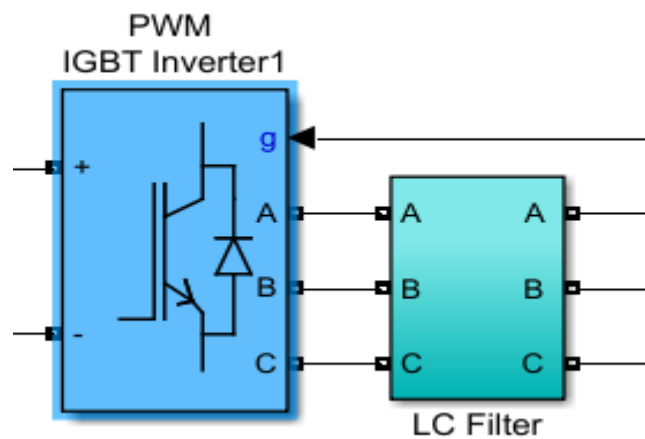

Figure 4.7: PWM Inverter

4.9 Main Circuit of Subsystem 2

Subsystem 2 also consists of PV modules, it has local load, battery storage system and the PID controlling mechanism, it has same power generation

capability like subsystem 1, it has local load of 4kw, it shares extra energy to subsystem 1 in this scenario because the generation capacity of the subsystem 1 is less than the load connected to it, so the extra amount of energy is shared to subsystem 1 by intelligent load management system.
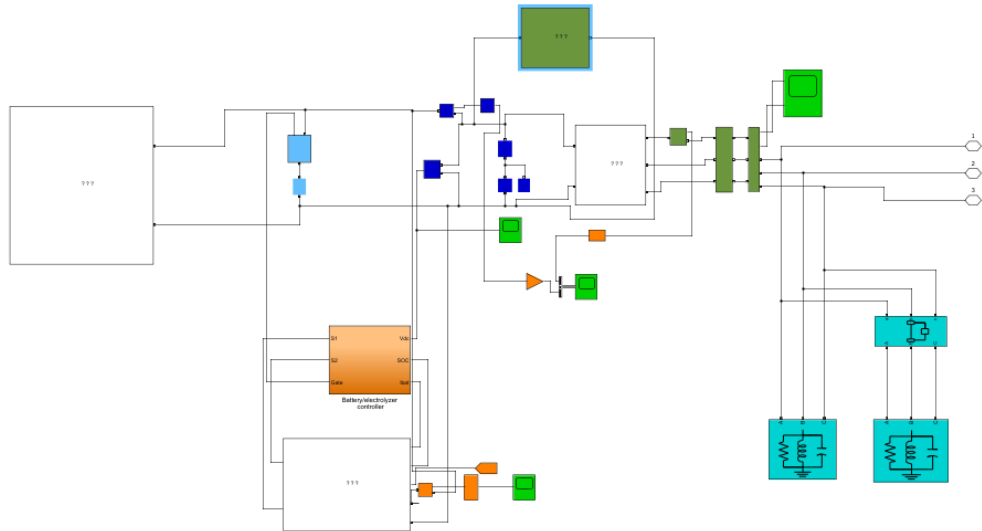
Figure 4.8: subsystem 2 PV Layout

4.10 Working of PV Subsystem 2
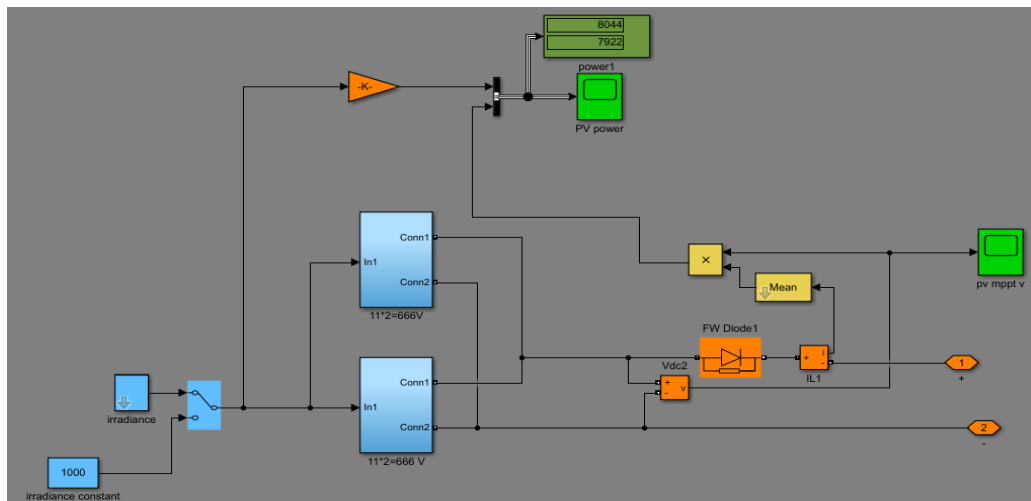
Figure 4.9: Circuit of PV subsystem 2

We have used two solar modules each produces 666 volts and they are connected to each other in parallel, here two values of solar irradiance, one is constant (1000) and other is variable (1000 at zero-time index and 850 at time index 2) are connected as input to solar arrays. A system is installed to track the

59

MPPT output of the solar modules, a free-wheeling diode is used to prevent the system from the reverse currents in order to prevent from system damage.

Figure 4.10: power generated by PV solar panels of subsystem

4.11 Methodology Description

Above pictures gives the stats of the generated power by PV modules, initially there is instability in the system, which is in transients condition, later this become stable in steady state operation. After 2 unit index on the x-axis, there is a little reduction in power due to the variability of the solar irradiance, and hence there is a bit less power obtained by the system, the mean value 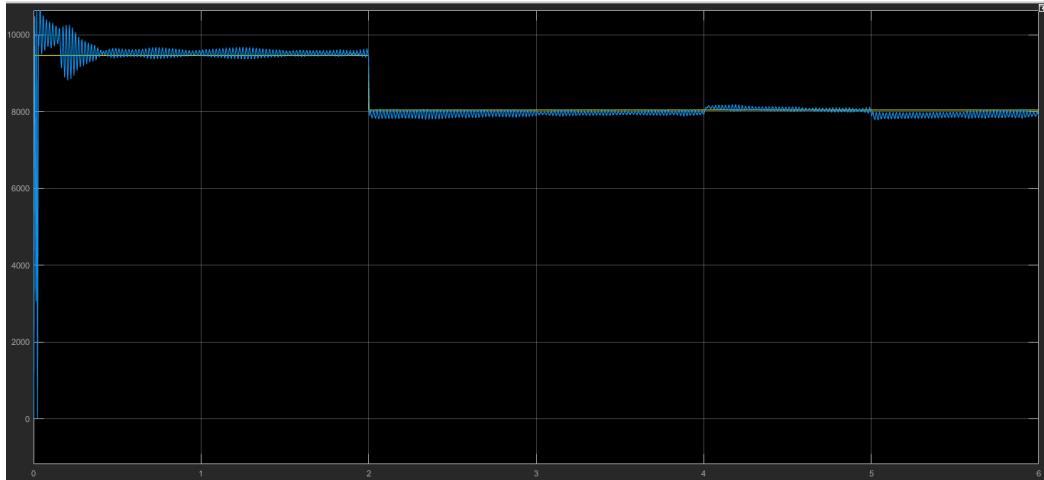of the power is about 9kw.it has same power generation capability like subsystem 1, it has local load of 4kw, it shares extra energy to subsystem 1 in this scenario because the generation capacity of the subsystem 1 is less than the load connected to it, so the extra amount of energy is shared to subsystem 1 by intelligent load management system.

4.12 Operation of battery System of Subsystem 2
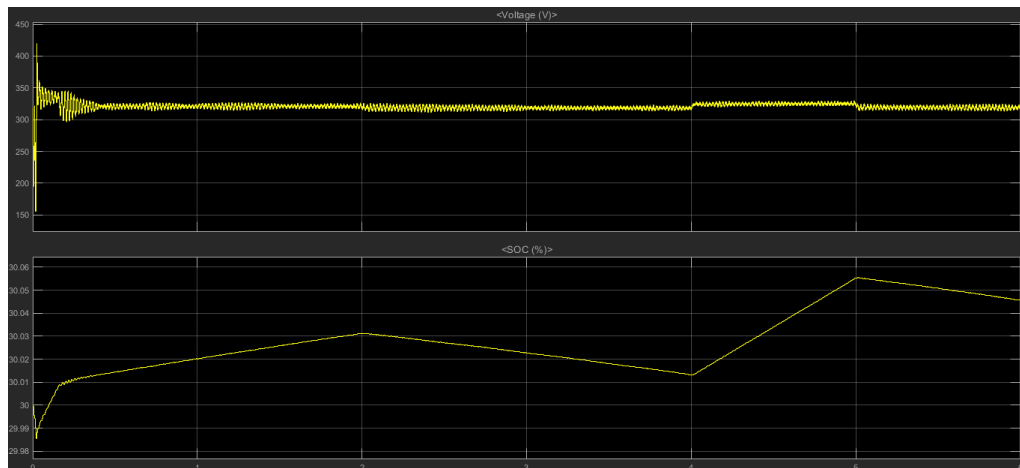
Figure 4.11: Battery voltage and SOC of Subsystem 2

The battery system also known as storage subsystem, is the backup system which is deployed to share the power to the system in case if generation resource is absent or there is extra load connected, so to cope this issue battery system is used as backup. this system is consisted of A battery bank, here we have used the 200 volts 6.5 Ampere hours Ni-MH battery, IGBT's for switching purposes, the battery power, state of charge and voltage monitor system, the battery system controlled by PID controller system (which will be discussed later), if the battery state of charge is below than the permissible limit the conventional method will be requested to supply the energy, so that the load will get the abrupt supply from the system, and battery will be recharged if there is excess power available on the system. There is an inductor L3 used in series with IGBT and battery for protection purposes.

In this specific scenario, subsystem 2,3 & 4 are sharing the extra power to subsystem 1 as it has extra local load which is 16kw. Subsystem 2 shares 4kw to subsystem 1 as well it charge local battery as we can observe from figure 4.10 as the SOC is improving to charge.

4.13 Operation of PID Controller

This is basic control system for switching process of battery to operate at different time according to the load and other resources. In this scenario PID is charging the battery because the system has less local load so PID drives the

system to charge the battery as well because the battery SOC of Subsystem 2 is below to the fully charge state.

Here, again two parameters of battery are taken into consideration that are:

- Voltage of battery

- Battery SOC

Initial SOC of battery 85% and response time 30 second that means whenever soc reach to 80%,it indicates that battery is fully charged.

This part is for voltage regulation of the battery this part will decide when voltage to increase and when to drop, whenever it senses load power is not compensated by other resources then it provides pulse to the switches s1 and s2, in this input to the PID is the comparison value of vdc and reference value.

PID works to achieve desired value. It provides switching pulses through s1 and s2 which in input to the MOSFET.

Battery management using SOC control system here input is soc of the current situation, in next step it is compared with some value of soc, that whenever the soc reached its minimum it provides pulses to s1 and s2 for recharging of battery.

Figure 4.12: Power Control by PID Controller

Subsystem 3 and 4 works exactly same as subsystem 2, which we have already discussed.

In this specific scenario, subsystem 2,3 & 4 are sharing the extra power to subsystem 1 as it has extra local load which is 16kw. All the three 2,3 & 4 are sharing 12kw, each subsystem shares 4kw to subsystem 1 to meet the load requirements. For further investigation we can check the storage subsystems of subsystem 3 and 4.
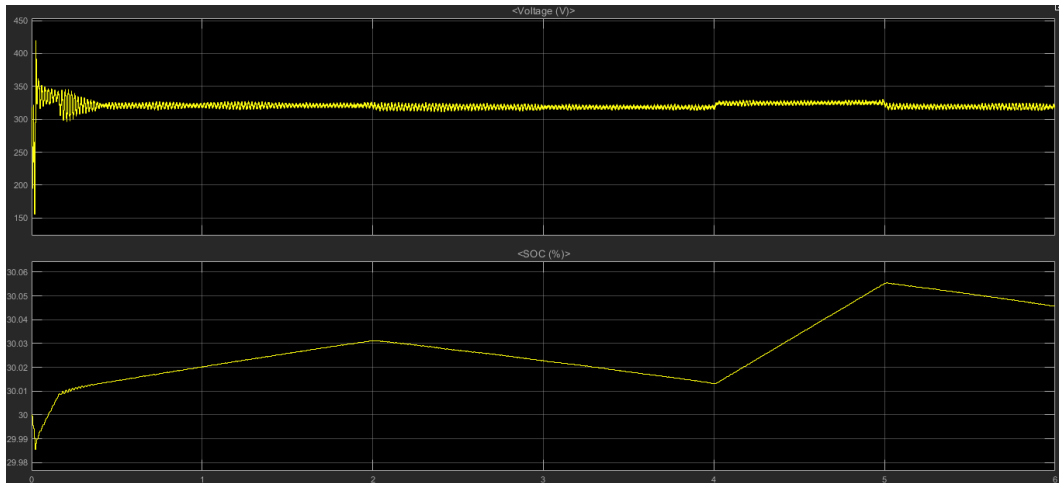
Figure 4.13: Battery voltage and SOC of Subsystem 3
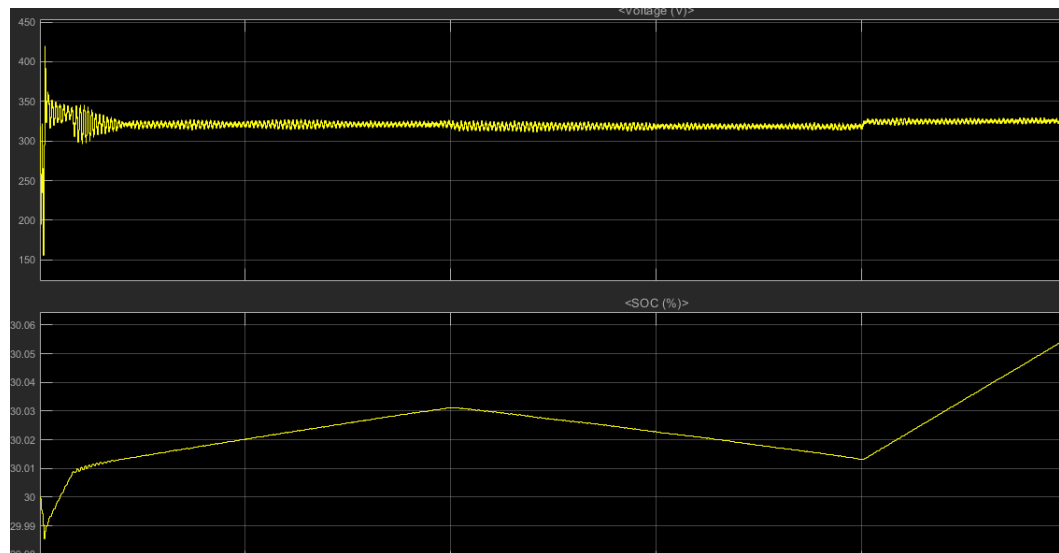
Figure 4.14: Battery voltage and SOC of Subsystem 4

4.14 Experiments and Results
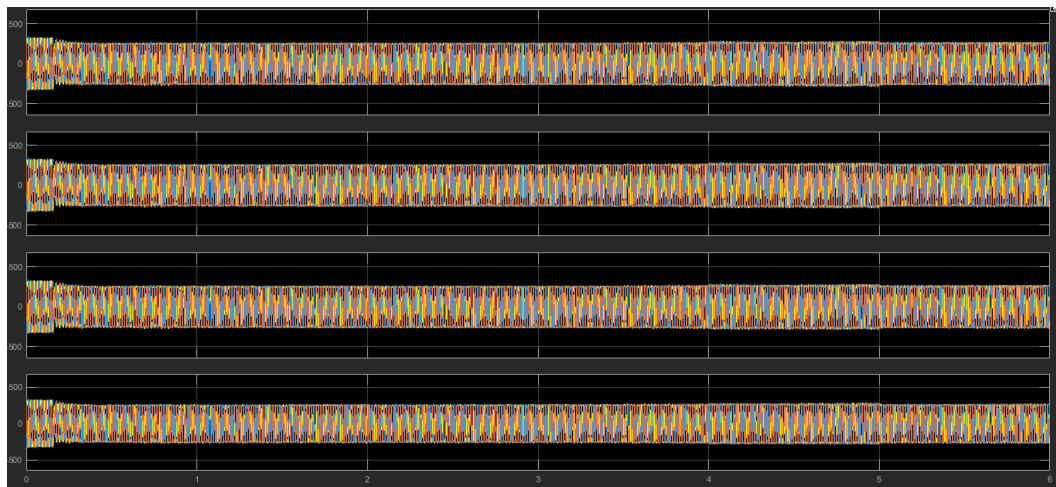
Figure 4.15: Voltages of all the subsystems
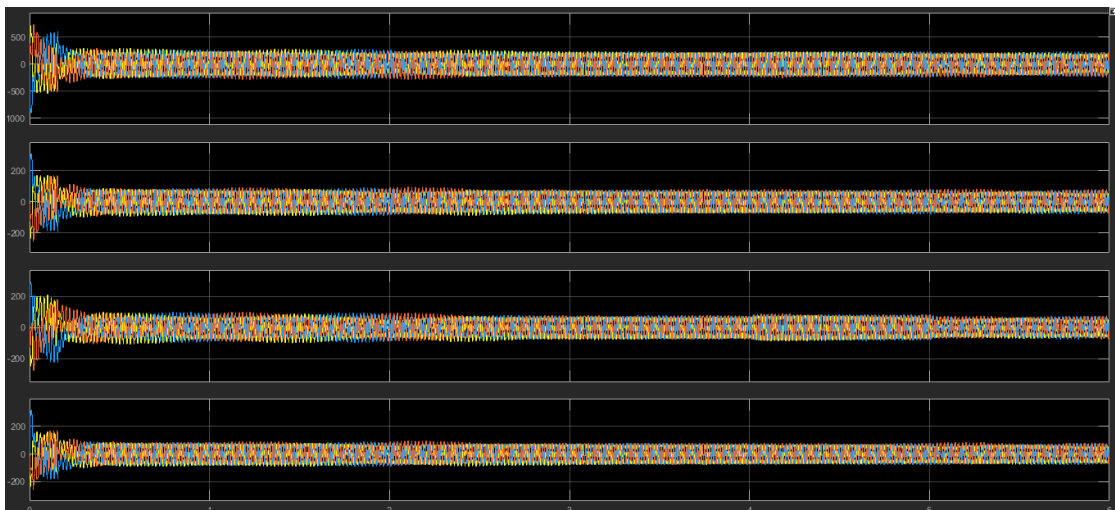
Figure 4.16: Voltages of all the subsystems
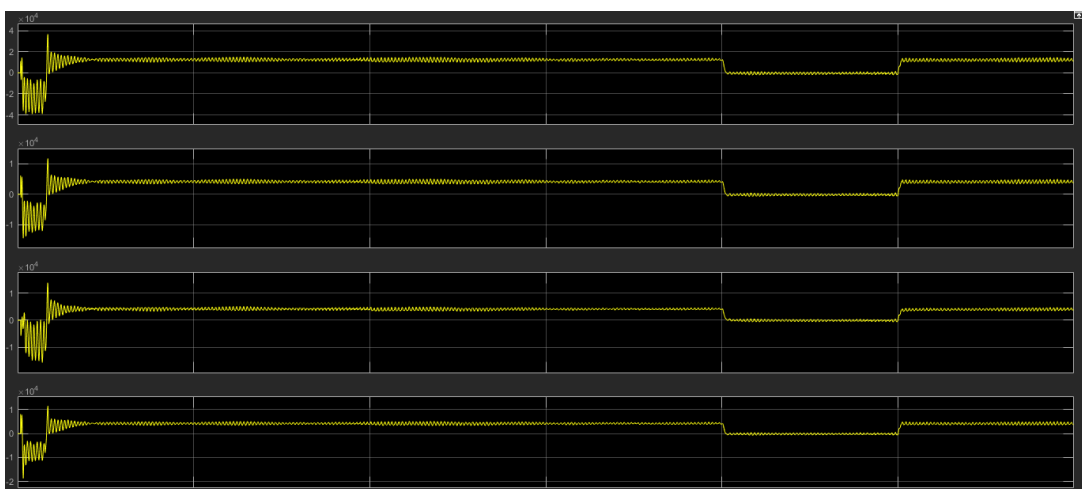
Figure 4.17: Currents of all the subsystems
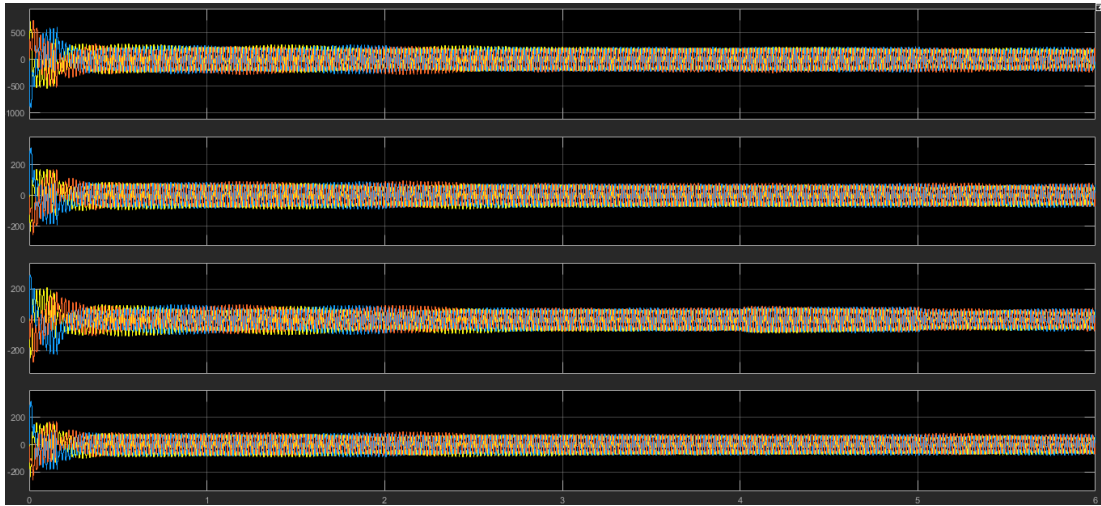
Figure 4.18: Power provided to loads of all the subsystems

5. CONCLUSION AND RECOMMENDATIONS

5.1 Conclusion

In this thesis, the solar micro-grids were examined, and the issues raised in them such as Operation method, maximum power point tracking, converter structure used, energy storage and various power management methods were mentioned. With the increasing use of batteries as energy storage and its use as a hybrid structure with solar arrays, in which the solar array and battery share a common inverter, the challenges of power management in solar microenvironment separate from the grid the types of solar independent units, battery independent and solar / battery units are mentioned. Providing an active power management approach and decentralized load distribution in separate micro-grid and battery-powered micro-grids is the main activity of this dissertation.

Initially, a single-phase micro-grid was considered and the decentralized control method for each grid unit was explained. However, this method is also applicable to three-phase micro-grids. Each microgrid unit consists of three parts: battery adapter control, PV adapter control and inverter control.

In order to implement decentralized power management, the performance of each unit was divided into six states and the manner of controlling each of these three sections in each status and status change situation was investigated. An algorithm was presented that allowed a unit to set its initial state when setting up and connecting to the micro-grid. Following are the necessary changes to implement the proposed method in standalone battery and PV units. The effect of resistance on inverter output impedance and line impedance was investigated in the proposed method and it was shown that the existence of resistance had the greatest effect on reactive power division and did not have much effect on the proposed active power management method. Finally, to evaluate the performance of the proposed method, simulation and practical results of a micro-network consisting of three single-phase hybrid units were presented. In

the simulations, the performance of the proposed power management method in different linear active load conditions, active and reactive load combination and nonlinear load was shown and in each case the effect of line impedance was investigated. In practical results only linear active load was considered. In the following chapter, the proposed method is extended to a single-phase / three-phase hybrid micro-network consisting of independent and hybrid PV units and batteries. In this three-phase micro-grid, in addition to six single-phase units, it can also accommodate two new states. Also, the automatic power transfer from phase to phase was investigated by three phase units. The simulation and practical results show that the proposed method for this micro-grid can also achieve the presented objectives.

5.2 Innovations In The Thesis

Innovations in this research include:

1. Providing a decentralized active power management approach for solar micro-grids, unlike other methods offered, is not limited to micro-grids consisting solely of independent solar and battery units.

2. In the proposed method, all limitations are considered including battery charge limitations, maximum PV power and inverter capacity.

3. In the proposed method, the maximum utilization of solar power is achieved and the SoC of the batteries is automatically balanced to the extent possible.

4. Although only the active power management has been investigated in the proposed method, it is applicable to a variety of reactive and nonlinear loads and can be combined with the methods presented in other studies to divide the reactive power and nonlinear loads by this method. The desired goals were achieved.

5. Application of the method presented in single phase / three phase hybrid micro-networks and the capability of automatic power transfer from phase to phase

5.3 Suggestions For Further Research

- Investigation of voltage imbalance and suggesting ways to reduce it in composite grid / three phase micro grid

- Investigating the capabilities of single phase / three phase hybrid network in connected mode

- Generalization of the proposed method to three-phase three-wire micro-networks

- Evaluation of various micro-network capabilities to compensate for major network errors in network-connected mode

- Use of a secondary controller to compensate for changes in the frequency and voltage range of the Drop method

REFERENCES

[1]   **Y. M. Chen, H. C. Wu, Y. C. Chen, K. Y. Lee, and S. S. Shyu,** "The AC line current regulation strategy for the grid-connected PV system," *IEEE Trans. Power Electron.*, vol. 25, no. 1, pp. 209–218, 2010, doi: 10.1109/TPEL.2009.2027238.

[2]   **M. Castilla, J. Miret, J. Matas, L. G. de Vicuña, and J. M. Guerrero,** "Control design guidelines for single-phase grid-connected photovoltaic inverters with damped resonant harmonic compensators," *IEEE Trans. Ind. Electron.*, vol. 56, no. 11, pp. 4492–4501, 2009, doi: 10.1109/TIE.2009.2017820.

[3]   **R. A. Mastromauro, M. Liserre, and A. Dell'Aquila,** "Control issues in single-stage photovoltaic systems: MPPT, current and voltage control," *IEEE Transactions on Industrial Informatics*, vol. 8, no. 2. pp. 241–254, May-2012, doi: 10.1109/TII.2012.2186973.

[4]   **M. Castilla, J. Miret, J. Matas, L. García de Vicuña, and J. M. Guerrero,** "Linear current control scheme with series resonant harmonic compensator for single-phase grid-connected photovoltaic inverters," *IEEE Trans. Ind. Electron.*, vol. 55, no. 7, pp. 2724–2733, Jul. 2008, doi: 10.1109/TIE.2008.920585.

[5]   **P. IEEE Standards** Coordinating Committee 21 on Fuel Cells, Institute of Electrical and Electronics Engineers., IEEE-SA Standards Board., and IEEE Xplore (Online service), *IEEE standard conformance test procedures for equipment interconnecting distributed resources with electric power systems*. Institute of Electrical and Electronics Engineers, 2005.

[6]   **F. Katiraei and M. R. Iravani,** "Power management strategies for a microgrid with multiple distributed generation units," *IEEE Trans. Power Syst.*, vol. 21, no. 4, pp. 1821–1831, Nov. 2006, doi: 10.1109/TPWRS.2006.879260.

[7]   **R. Ramakumar and S. Member IEEE,** "at the moment of switching off and subsequently the free oscilla¬ tion that follows From Figs 1a and 1b it Renewable Energy Sources and Developing Countries," 1983.

[8]   **H. Patel and V. Agarwal,** "Maximum power point tracking scheme for PV systems operating under partially shaded conditions," *IEEE Trans. Ind. Electron.*, vol. 55, no. 4, pp. 1689–1698, Apr. 2008, doi: 10.1109/TIE.2008.917118.

[9]   **N. Femia, G. Petrone, G. Spagnuolo, and M. Vitelli**, "Optimization of perturb and observe maximum power point tracking method," *IEEE Trans. Power Electron.*, vol. 20, no. 4, pp. 963–973, Jul. 2005, doi: 10.1109/TPEL.2005.850975.

[10]   **D. Sera, R. Teodorescu, J. Hantschel, and M. Knoll,** "Optimized maximum power point tracker for fast-changing environmental conditions," *IEEE Trans. Ind. Electron.*, vol. 55, no. 7, pp. 2629–2637, Jul. 2008, doi: 10.1109/TIE.2008.924036.

[11]   **Y. H. Ji, D. Y. Jung, J. G. Kim, J. H. Kim, T. W. Lee, and C. Y. Won,** "A

real maximum power point tracking method for mismatching compensation in PV array under partially shaded conditions," *IEEE Trans. Power Electron.*, vol. 26, no. 4, pp. 1001–1009, 2011, doi: 10.1109/TPEL.2010.2089537.

[12] **K. Ishaque and Z. Salam,** "A deterministic particle swarm optimization maximum power point tracker for photovoltaic system under partial shading condition," *IEEE Trans. Ind. Electron.*, vol. 60, no. 8, pp. 3195–3206, 2013, doi: 10.1109/TIE.2012.2200223.

[13] **B. Subudhi and R. Pradhan,** "A comparative study on maximum power point tracking techniques for photovoltaic power systems," *IEEE Trans. Sustain. Energy*, vol. 4, no. 1, pp. 89–98, 2013, doi: 10.1109/TSTE.2012.2202294.

[14] **M. Bragard, N. Soltau, S. Thomas, and R. W. De Doncker,** "The balance of renewable sources and user demands in grids: Power electronics for modular battery energy storage systems," *IEEE Trans. Power Electron.*, vol. 25, no. 12, pp. 3049–3056, 2010, doi: 10.1109/TPEL.2010.2085455.

[15] **L. Liu, H. Li, Z. Wu, and Y. Zhou,** "A cascaded photovoltaic system integrating segmented energy storages with self-regulating power allocation control and wide range reactive power compensation," *IEEE Trans. Power Electron.*, vol. 26, no. 12, pp. 3545–3559, 2011, doi: 10.1109/TPEL.2011.2168544.

[16] **H. Zhou, T. Bhattacharya, D. Tran, T. S. T. Siew, and A. M. Khambadkone**, "Composite energy storage system involving battery and ultracapacitor with dynamic energy management in microgrid applications," *IEEE Trans. Power Electron.*, vol. 26, no. 3, pp. 923–930, 2011, doi: 10.1109/TPEL.2010.2095040.

[17] **H. Beltran, E. Bilbao, E. Belenguer, I. Etxeberria-Otadui, and P. Rodriguez**, "Evaluation of storage energy requirements for constant production in PV power plants," *IEEE Trans. Ind. Electron.*, vol. 60, no. 3, pp. 1225–1234, 2013, doi: 10.1109/TIE.2012.2202353.

[18] **H. Fakham, D. Lu, and B. Francois,** "Power control design of a battery charger in a hybrid active PV generator for load-following applications," *IEEE Trans. Ind. Electron.*, vol. 58, no. 1, pp. 85–94, Jan. 2011, doi: 10.1109/TIE.2010.2062475.

[19] **S. Teleke, M. E. Baran, S. Bhattacharya, and A. Q. Huang,** "Rule-based control of battery energy storage for dispatching intermittent renewable sources," *IEEE Trans. Sustain. Energy*, vol. 1, no. 3, pp. 117–124, Oct. 2010, doi: 10.1109/TSTE.2010.2061880.

[20] **Z. Wang, S. Fan, Y. Zheng, and M. Cheng,** "Design and analysis of a CHB converter based PV-battery hybrid system for better electromagnetic compatibility," *IEEE Trans. Magn.*, vol. 48, no. 11, pp. 4530–4533, 2012, doi: 10.1109/TMAG.2012.2198912.

[21] **B. Ge *et al.*,** "An energy-stored quasi-Z-source inverter for application to photovoltaic power system," *IEEE Trans. Ind. Electron.*, vol. 60, no. 10, pp. 4468–4481, 2013, doi: 10.1109/TIE.2012.2217711.

[22] **J. Liu, S. Jiang, D. Cao, and F. Z. Peng,** "A digital current control of quasi-Z-source inverter with battery," *IEEE Trans. Ind. Informatics*, vol. 9, no. 2, pp. 928–937, May 2013, doi: 10.1109/TII.2012.2222653.

[23] **R. González, J. López, P. Sanchis, and L. Marroyo,** "Transformerless inverter for single-phase photovoltaic systems," *IEEE Trans. Power Electron.*, vol. 22, no. 2, pp. 693–697, Mar. 2007, doi: 10.1109/TPEL.2007.892120.

[24] T. Kerekes, R. Teodorescu, P. Rodríguez, G. Vázquez, and E. Aldabas, "A New high-efficiency single-phase transformerless PV inverter topology," *IEEE Trans. Ind. Electron.*, vol. 58, no. 1, pp. 184–191, Jan. 2011, doi: 10.1109/TIE.2009.2024092.

[25] **B. Gu, J. Dominic, J. S. Lai, C. L. Chen, T. Labella, and B. Chen,** "High reliability and efficiency single-phase transformerless inverter for grid-connected photovoltaic systems," *IEEE Trans. Power Electron.*, vol. 28, no. 5, pp. 2235–2245, 2013, doi: 10.1109/TPEL.2012.2214237.

[26] **M. C. Cavalcanti, K. C. De Oliveira, A. M. De Farias, F. A. S. Neves, G. M. S. Azevedo, and F. C. Camboim,** "Modulation techniques to eliminate leakage currents in transformerless three-phase photovoltaic systems," *IEEE Trans. Ind. Electron.*, vol. 57, no. 4, pp. 1360–1368, Apr. 2010, doi: 10.1109/TIE.2009.2029511.

[27] **C. C. Hou, C. C. Shih, P. T. Cheng, and A. M. Hava,** "Common-mode voltage reduction pulsewidth modulation techniques for three-phase grid-connected converters," *IEEE Trans. Power Electron.*, vol. 28, no. 4, pp. 1971–1979, Apr. 2013, doi: 10.1109/TPEL.2012.2196712.

[28] **Y. Tang, P. C. Loh, P. Wang, F. H. Choo, and F. Gao,** "Exploring inherent damping characteristic of LCL-filters for three-phase grid-connected voltage source inverters," *IEEE Trans. Power Electron.*, vol. 27, no. 3, pp. 1433–1443, 2012, doi: 10.1109/TPEL.2011.2162342.

[29] **P. C. Loh and D. G. Holmes,** "Analysis of multiloop control strategies for LC/CL/LCL-filtered voltage-source and current-source inverters," *IEEE Trans. Ind. Appl.*, vol. 41, no. 2, pp. 644–654, Mar. 2005, doi: 10.1109/TIA.2005.844860.

[30] **W. Wu, Y. He, and F. Blaabjerg,** "An LLCL power filter for single-phase grid-tied inverter," *IEEE Trans. Power Electron.*, vol. 27, no. 2, pp. 782–789, 2012, doi: 10.1109/TPEL.2011.2161337.

[31] "Comparison of active and passive damping methods for application in high power active power filter with LCL-filter."

[32] **E. Wu and P. W. Lehn,** "Digital current control of a voltage source converter with active damping of LCL resonance," *IEEE Trans. Power Electron.*, vol. 21, no. 5, pp. 1364–1373, 2006, doi: 10.1109/TPEL.2006.880271.

[33] **J. Dannehl, M. Liserre, and F. W. Fuchs,** "Filter-based active damping of voltage source converters with LCL filter," *IEEE Trans. Ind. Electron.*, vol. 58, no. 8, pp. 3623–3633, Aug. 2011, doi: 10.1109/TIE.2010.2081952.

[34] **J. Dannehl, F. W. Fuchs, S. Hansen, and P. B. Thøgersen,** "Investigation of active damping approaches for PI-based current control of grid-connected pulse width modulation converters with LCL filters," *IEEE Trans. Ind. Appl.*, vol. 46, no. 4, pp. 1509–1517, Jul. 2010, doi: 10.1109/TIA.2010.2049974.

[35] **W. Wu, Y. He, T. Tang, and F. Blaabjerg,** "A new design method for the passive damped LCL and LLCL filter-based single-phase grid-tied inverter," *IEEE Trans. Ind. Electron.*, vol. 60, no. 10, pp. 4339–4350, 2013, doi: 10.1109/TIE.2012.2217725.

[36] **H. Mahmood, D. Michaelson, and J. Jiang,** "Decentralized Power Management of a PV/Battery Hybrid Unit in a Droop-Controlled Islanded Microgrid," *IEEE Trans. Power Electron.*, vol. 30, no. 12, pp. 7215–7229, Dec. 2015, doi: 10.1109/TPEL.2015.2394351.

[37] **M. Hamzeh, A. Ghazanfari, H. Mokhtari, and H. Karimi,** "Integrating hybrid power source into an Islanded MV microgrid using CHB multilevel

inverter under unbalanced and nonlinear load conditions," *IEEE Trans. Energy Convers.*, vol. 28, no. 3, pp. 643–651, 2013, doi: 10.1109/TEC.2013.2267171.

[38] **I. Y. Chung, W. Liu, D. A. Cartes, E. G. Collins, and S. Il Moon,** "Control methods of inverter-interfaced distributed generators in a microgrid system," in *IEEE Transactions on Industry Applications*, 2010, vol. 46, no. 3, pp. 1078–1088, doi: 10.1109/TIA.2010.2044970.

[39] **J. He and Y. W. Li,** "An enhanced microgrid load demand sharing strategy," *IEEE Trans. Power Electron.*, vol. 27, no. 9, pp. 3984–3995, 2012, doi: 10.1109/TPEL.2012.2190099.

[40] **B. Belvedere, M. Bianchi, A. Borghetti, C. A. Nucci, M. Paolone, and A. Peretto,** "A microcontroller-based power management system for standalone microgridswith hybrid power supply," *IEEE Trans. Sustain. Energy*, vol. 3, no. 3, pp. 422–431, 2012, doi: 10.1109/TSTE.2012.2188654.

[41] **Y. K. Chen, Y. C. Wu, C. C. Song, and Y. S. Chen,** "Design and implementation of energy management system with fuzzy control for DC microgrid systems," *IEEE Trans. Power Electron.*, vol. 28, no. 4, pp. 1563–1570, Apr. 2013, doi: 10.1109/TPEL.2012.2210446.

[42] **K. T. Tan, P. L. So, Y. C. Chu, and M. Z. Q. Chen,** "Coordinated Control and Energy Management of Distributed Generation Inverters in a Microgrid," *IEEE Trans. Power Deliv.*, vol. 28, no. 2, pp. 704–713, 2013, doi: 10.1109/TPWRD.2013.2242495.

[43] **K. T. Tan, X. Y. Peng, P. L. So, Y. C. Chu, and M. Z. Q. Chen,** "Centralized control for parallel operation of distributed generation inverters in microgrids," *IEEE Trans. Smart Grid*, vol. 3, no. 4, pp. 1977–1987, 2012, doi: 10.1109/TSG.2012.2205952.

[44] **J. Y. Kim *et al.*,** "Cooperative control strategy of energy storage system and microsources for stabilizing the microgrid during islanded operation," *IEEE Trans. Power Electron.*, vol. 25, no. 12, pp. 3037–3048, 2010, doi: 10.1109/TPEL.2010.2073488.

[45] **H. Kanchev, D. Lu, F. Colas, V. Lazarov, and B. Francois,** "Energy management and operational planning of a microgrid with a PV-based active generator for smart grid applications," *IEEE Trans. Ind. Electron.*, vol. 58, no. 10, pp. 4583–4592, 2011, doi: 10.1109/TIE.2011.2119451.

[46] **E. Serban and H. Serban,** "A control strategy for a distributed power generation microgrid application with voltage- and current-controlled source converter," *IEEE Trans. Power Electron.*, vol. 25, no. 12, pp. 2981–2992, 2010, doi: 10.1109/TPEL.2010.2050006.

[47] **D. Wu, F. Tang, T. Dragicevic, J. C. Vasquez, and J. M. Guerrero,** "Autonomous active power control for islanded AC microgrids with photovoltaic generation and energy storage system," *IEEE Trans. Energy Convers.*, vol. 29, no. 4, pp. 882–892, 2014, doi: 10.1109/TEC.2014.2358612.

[48] **J. G. De Matos, F. S. F. E Silva, and L. A. S. Ribeiro,** "Power control in AC isolated microgrids with renewable energy sources and energy storage systems," *IEEE Trans. Ind. Electron.*, vol. 62, no. 6, pp. 3490–3498, Jun. 2015, doi: 10.1109/TIE.2014.2367463.

[49] **A. Urtasun, E. L. Barrios, P. Sanchis, and L. Marroyo,** "Frequency-based energy-management strategy for stand-alone systems with distributed battery storage," *IEEE Trans. Power Electron.*, vol. 30, no. 9, pp. 4794–4808, Sep. 2015, doi: 10.1109/TPEL.2014.2364861.

[50]   D. Wu, F. Tang, T. Dragicevic, J. C. Vasquez, and J. M. Guerrero, "A Control Architecture to Coordinate Renewable Energy Sources and Energy Storage Systems in Islanded Microgrids," *IEEE Trans. Smart Grid*, vol. 6, no. 3, pp. 1156–1166, 2015, doi: 10.1109/TSG.2014.2377018.

[51]   H. Mahmood, D. Michaelson, and J. Jiang, "Strategies for Independent Deployment and Autonomous Control of PV and Battery Units in Islanded Microgrids," *IEEE J. Emerg. Sel. Top. Power Electron.*, vol. 3, no. 3, pp. 742–755, 2015, doi: 10.1109/JESTPE.2015.2413756.

[52]   K. De Brabandere, B. Bolsens, J. Van Den Keybus, A. Woyte, J. Driesen, and R. Belmans, "A voltage and frequency droop control method for parallel inverters," *PESC Rec. - IEEE Annu. Power Electron. Spec. Conf.*, vol. 4, no. 4, pp. 2501–2507, 2004, doi: 10.1109/PESC.2004.1355222.

[53]   S. K. Kim, J. H. Jeon, C. H. Cho, J. B. Ahn, and S. H. Kwon, "Dynamic modeling and control of a grid-connected hybrid generation system with versatile power transfer," *IEEE Trans. Ind. Electron.*, vol. 55, no. 4, pp. 1677–1688, 2008, doi: 10.1109/TIE.2007.907662.

[54]   T. Hirose and H. Matsuo, "Standalone hybrid wind-solar power generation system applying dump power control without dump load," *IEEE Trans. Ind. Electron.*, vol. 59, no. 2, pp. 988–997, 2012, doi: 10.1109/TIE.2011.2159692.

[55]   H. C. Chiang, T. T. Ma, Y. H. Cheng, J. M. Chang, and W. N. Chang, "Design and implementation of a hybrid regenerative power system combining grid-tie and uninterruptible power supply functions," *IET Renew. Power Gener.*, vol. 4, no. 1, pp. 85–99, 2010, doi: 10.1049/iet-rpg.2009.0033.

[56]   J. A. P. Lopes, C. L. Moreira, and A. G. Madureira, "Defining control strategies for analysing microgrids islanded operation," *2005 IEEE Russ. Power Tech, PowerTech*, vol. 21, no. 2, pp. 916–924, 2005, doi: 10.1109/PTC.2005.4524548.

[57]   I. J. Balaguer, Q. Lei, S. Yang, U. Supatti, and F. Z. Peng, "Control for grid-connected and intentional islanding operations of distributed power generation," *IEEE Trans. Ind. Electron.*, vol. 58, no. 1, pp. 147–157, 2011, doi: 10.1109/TIE.2010.2049709.

[58]   J. Matas, M. Castilla, L. G. De Vicuña, J. Miret, and J. C. Vasquez, "Virtual impedance loop for droop-controlled single-phase parallel inverters using a second-order general-integrator scheme," *IEEE Trans. Power Electron.*, vol. 25, no. 12, pp. 2993–3002, 2010, doi: 10.1109/TPEL.2010.2082003.

[59]   J. C. Vasquez, J. M. Guerrero, M. Savaghebi, J. Eloy-Garcia, and R. Teodorescu, "Modeling, analysis, and design of stationary-reference-frame droop-controlled parallel three-phase voltage source inverters," *IEEE Trans. Ind. Electron.*, vol. 60, no. 4, pp. 1271–1280, 2013, doi: 10.1109/TIE.2012.2194951.

[60]   F. De Bosio, L. A. De Souza Ribeiro, M. Savaghebi, J. C. Vasquez, and J. M. Guerrero, "Control design of VSIs to enhance transient performance in microgrids," *2016 18th Eur. Conf. Power Electron. Appl. EPE 2016 ECCE Eur.*, pp. 1–8, 2016, doi: 10.1109/EPE.2016.7695496.

[61]   X. Lu, K. Sun, J. M. Guerrero, J. C. Vasquez, and L. Huang, "Double-quadrant state-of-charge-based droop control method for distributed energy storage systems in autonomous DC Microgrids," *IEEE Trans. Smart Grid*, vol. 6, no. 1, pp. 147–157, 2015, doi: 10.1109/TSG.2014.2352342.

[62]   J. M. Guerrero, J. C. Vasquez, J. Matas, L. G. De Vicuña, and M.

Castilla, "Hierarchical control of droop-controlled AC and DC microgrids - A general approach toward standardization," *IEEE Trans. Ind. Electron.*, vol. 58, no. 1, pp. 158–172, 2011, doi: 10.1109/TIE.2010.2066534.

[63]   **M. Savaghebi, A. Jalilian, J. C. Vasquez, and J. M. Guerrero,** "Secondary control scheme for voltage unbalance compensation in an Islanded droop-controlled microgrid," *IEEE Trans. Smart Grid*, vol. 3, no. 2, pp. 797–807, 2012, doi: 10.1109/TSG.2011.2181432.

RESUME

Name Surname: Hasibullah Shams
Place and Date of Birth: Afghanistan, 23rd of December 1993
Email: hasibullahshams@stu.aydin.edu.tr ,   hasib.shams77@gmail.com

EDUCATION:
- **Bachelor:** December 2014, Kabul University, Kabul, Afghanistan, Physics.
- **Masters:** April 2020, Istanbul Aydin University, Istanbul, Turkey, Electrical & Electronics Engineering.

CERTIFICATES
- C++
- COMPUTER NETWORKING
  - Achieved (**ICDL/ECDL**) International computer Driving License. (**2012**)
  - **IT** Certificate from **ITCK** Center of Kabul University
    - **Hardware Basics**
    - **Operating System**
    - **Networking Basics**
    - **Linux Basics**
    - **Web designing**
    - **Advanced Networking**
- IELTS
- Deutsch A1
- TÖMER C1

WORKSHOPS & SEMINARS
- Essential of Occupational Safety & Health (**EOSH**), Ankara, Turkey, 2019
- Student Satisfaction Workshop, (**IAU**), Istanbul, Turkey, April 2019

PROFESSIONAL EXPERIENCE:
- Two-year Data Manager & Data Analyses coordinator   **Kabul, Afghanistan**
- Faculty Admin **IT** Assistant   **Kabul, Afghanistan**
- Freelance English Teacher & Interpreter   **Istanbul, Turkey**
- Sales Representative **ICB.CAPITAL**   **Istanbul, Turkey & North Cypris**